



## Optimal control of organic matter applications

Thibaut Putelat<sup>a,\*</sup>, Andrew P. Whitmore<sup>a</sup>

<sup>a</sup> Net Zero and Resilient Farming, Rothamsted Research, Harpenden AL5 2JQ, UK

### ARTICLE INFO

#### Keywords:

Response curve  
Optimal control  
Organic matter  
Fertiliser  
Carbon  
Long term experiment

### ABSTRACT

Organic matter amendments appear to increase yield, but need to be sustained, as yield decreases when amendments cease. Here we mathematically devise optimal strategies for organic matter applications that take account of how quickly, in years of application, yields build up with amendments and how long these benefits persist. The empirical idea of a nutrient response curve is used and extended to include more than a single nutrient input as well as the effect of yield-enhancing factors such as organic matter that endure for more than one year. Nonlinear regression is used for the selection and the parameter identification for a reciprocal response curve working with a dataset from Rothamsted's Woburn organic manuring long term experiment. Such a response curve is then treated analytically to develop economically optimum applications over a period of time. A simple static case is developed first and is shown to be equivalent to the well-known break-even ratio (BER) used in nitrogen fertiliser guidance by the Agricultural and Horticultural Development Board in the UK. The mathematical technique of optimal control is then employed to deduce dynamic strategies where the application of an amendment may change from year to year and for different time frames. Because this empirical modelling methodology can appear complex, we infer a rule-of-thumb for an equilibrium level of yield-enhancement rather like the equilibrium level of organic carbon that builds up over several years. This yield-enhancing power of organic matter is somewhat variable and probably does not persist in soil for as long as the organic matter from which it derives. It appears beneficial to apply amendments at a constant rate for much of the time-frame of interest but to begin with a large application to raise the fertility to the yield-enhancement equilibrium. After a transition year with reduced amendments, applications of organic matter are stopped for the final five years with the example amendment studied, farmyard manure. These conclusions depend on the persistence of the yield-enhancing power of organic matter in soil associated with the soil organic carbon kinetics.

### 1. Introduction

Chemical fertilisers are held responsible for all manner of current environmental ills (UNEP, 2022). However, without fertiliser crop yields may be expected to decrease, which threatens future food security (Stewart et al., 2005; Stewart and Roberts, 2012). Moreover, if yield levels become uneconomic as a result of a change in management practices, the area sown to some crops such as oilseed rape could drop dramatically (Dewar, 2017). Balancing such contradictory aims makes agricultural sustainability quite challenging.

A possible remedy to this issue may be to rely on organic amendments, such as manure and compost, whose many benefits for agricultural and soil health are becoming increasingly recognised (Johnston et al., 2009). Like fertiliser, organic amendments can increase yield so they could partly replace artificial nitrogen (N). The yield enhancing power of organic amendments follows from both physical and chemical

processes by improving both nutrient availability and physical attributes such as soil structure and water retention (Johnston et al., 2009; Thomas et al., 2019; Neal et al., 2020; Albano et al., 2022). In this article, our approach empirically bypasses these complications from relying on the concept of crop nutrient response curves (Greenwood et al., 1971; Thornley, 1978; George, 1984).

For a given crop, nutrient response curves map crop yield onto nutrient doses and are usually obtained from field experiments where different plots receive different rates of fertiliser application. As such, characterising crop nutrient demand, empirical response curves correspond to production functions that integrate the whole chain of processes involved in the soil-plant-atmosphere system throughout a growing season (Thornley and Johnson, 1990).

Nutrient response curves underpin guidance on the use of N fertiliser for a wide range of crops (e.g., RB209, 2022). Guidance is usually given in terms of profit maximisation and relies on the concept of the

\* Corresponding author.

E-mail address: [thibaut.putelat@rothamsted.ac.uk](mailto:thibaut.putelat@rothamsted.ac.uk) (T. Putelat).

<https://doi.org/10.1016/j.eja.2022.126713>

Received 17 July 2022; Received in revised form 25 November 2022; Accepted 26 November 2022

Available online 6 December 2022

1161-0301/© 2022 The Author(s). Published by Elsevier B.V. This is an open access article under the CC BY license (<http://creativecommons.org/licenses/by/4.0/>).

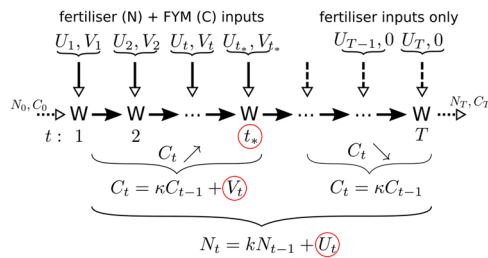


**Fig. 1.** Schematic of the optimal control theory (OCT) for fertiliser and organic amendment applications. Here, with the view of maximising profit, OCT is used for a crop (e.g. wheat) grown continuously over  $T$  seasons and whose yield response to nutrient inputs and organic amendments is known. It allows determining the schedule and application rates of nitrogen ( $U_t$ ) and organic matter ( $V_t$ ), such as farmyard manure (FYM), in accord with the yearly dynamics of soil nitrogen  $N_t$  and carbon  $C_t$  assumed to be governed by simple linear and uncoupled recurrence equations dynamics. It is predicted that organic amendments should be discontinued after a critical discontinuation time  $t_w$ , which depends on the application cost of organic amendments and the carry-over constant  $\kappa$  of carbon.

break-even ratio (BER), which defines the on-farm economic optimum nutrient (nitrogen) rate. Maximum profit is reached when the cost of fertiliser (i.e. marginal cost)  $c\Delta N$  equates the crop value (i.e. marginal revenue)  $p\Delta Y$ , where  $c$  is the unit cost (in  $\text{£}/\text{kg N}$ ) of fertiliser and  $p$  is the price (in  $\text{£}/\text{t}$ ) of the crop;  $\Delta Y$  representing the small increment in yield associated with a small increment in nitrogen input  $\Delta N$ . It follows that the BER value is defined as the ratio  $c/p$ . The corresponding BER nitrogen rate then is the rate at which the slope of the response curve solves the equation

$$\frac{dY}{dN} = \frac{c}{p} := \lim_{\Delta N \rightarrow 0} \frac{\Delta Y}{\Delta N} \quad (1)$$

Such a principle can be extended to other nutrients like phosphorus  $P$  and potassium  $K$  (Barnes et al., 1976; Thornley, 1976, 1978).

Here we go further and answer the question of how to apply inputs such as organic matter whose benefits persist for more than one year. Note that soil carbon is not seen as a plant nutrient, but rather as a proxy (or hidden variable) to quantify the yield enhancing properties that result from amendment. And, because amendments such as manure or compost can also be in short supply, we seek optimal means for how to apply  $N$  alongside annual applications of organic amendments that take account of how quickly yields build up with amendment, how long these benefits persist, and how  $N$  fertiliser might be reduced in such a way as to increase NUE (nutrient use efficiency). With this view in mind and in contrast to the BER reasoning, our approach will follow the time evolution of soil fertility.

To this end, we use discrete optimal control theory (Sage and White, 1977; Sethi, 2019), which brings a rational basis for combining applications of inorganic fertiliser and organic matter to a sequence of crops grown in consecutive seasons that ensures maximum profit from crop production. Our methodology thus generalises into a dynamic form the break-even ratio used for annual nitrogen fertiliser recommendations. In this paper, we show how this methodology can be used to develop efficient time-dependent  $N$  and OM guidance that is both sustainable and optimal. Examples of the method in action will be presented using datasets from a long-term experiment with respect to  $N$  and organic matter. In our approach, we do not aim at describing in detail the dynamics of the nitrogen and carbon cycling. Rather we wish to capture the essence of the problem from a parsimonious and empirical approach with the right level of model complexity in view of farming applications and the field experiment observations at our disposal.

## 2. Materials and methods

### 2.1. Overview

Technically, the dynamic methodology that we propose in this article computes economically optimal strategies, over a finite period of time, for the combined applications of organic matter and fertiliser in each season. In practice, our framework is based on a generalisation of response curves defined analytically as inverse polynomials inspired by Balmukand (1928), Greenwood et al. (1971) and Thornley (1978), because negative exponential or linear-plus-exponential ('lexp') response curve models (George, 1984) do not extend so readily to include more than a single input or a yield-enhancing factor such as organic matter that endure for more than one year. However, a modification of 'lexp' model is proposed in B and showed to perform no better than the inverse polynomial model presented below in terms of fitting a long term experiment dataset from the Woburn Organic Manuring experiment (Mattingly, 1974).

In contrast with a static constrained optimisation scheme, where the constraints are usually algebraic equations or inequalities (Mangasarian, 1969), optimal control theory is a dynamical system optimisation technique whose constraints are given by evolution equations (Pontryagin, 1987; Sage and White, 1977; Sethi, 2019). Our approach here is very much simplified in the sense that we will formulate our problem in a discrete fashion as a sequence of a finite number of seasons describing the yearly evolution of the soil nitrogen and carbon contents (Fig. 1).

Conceptually, optimal control theory needs us to clearly distinguish between two types of variables, namely, state variables and control variables. In our case, state variables correspond to the soil nitrogen and carbon contents, whereas control variables represent the artificial nitrogen and yield-enhancing carbon inputs related the amounts of fertiliser and organic amendment added each season. Note that this requires us to question the theoretical nature of what a response curve represents. Here, a response curve will be a multivariate function of the state variables, i.e. the soil mineral nitrogen and carbon, and not a function of the  $N$  and  $C$  inputs as assumed in a static BER type of approach. The response curve and recurrence equations parameter identification that we have developed takes care of this distinction between the variables (Sec. 2.3). Finally, a third type of variable known as a Lagrange multiplier, also referred to as co-state, needs to be introduced to ensure that the problem constraints are satisfied. In turn we will derive two additional recurrence equations determining the evolution of the two Lagrange multipliers associated with the changes in soil carbon and soil mineral nitrogen. That is to say we allow some organic  $C$  and mineral  $N$  to be retained in soil from one year to the next. These Lagrange multipliers are usually interpreted as shadow prices (Intriligator, 1971; Clark, 1976; Chiang, 1984; Sethi, 2019), bringing a monetary value to the gain or loss of soil fertility.

Because identification of the parameters of the response curve is a somewhat different issue from optimal control theory, we start by presenting a method to fit a four-parameter response curve (Eq. (3)), which includes the dynamics of carbon. The results are presented in Sec. 3.1. To do this we require data and have used several years of yield data from one of the Rothamsted long-term experiments (Macdonald et al., 2019). With the parameterised curves, we demonstrate the limitations of a BER-type static analysis using classical optimisation techniques and go on to develop a dynamic approach to the use of organic amendments over more than one year using optimal control theory.

### 2.2. The Woburn manuring experiment

The Woburn Organic Manuring experiment managed by Rothamsted Research (Mattingly, 1974) was started in 1964 to compare, within a single long-term experiment, most of the treatments to increase soil organic matter which had previously been tested in separate experiments at Woburn leading up to the 1960 s. It continues to this day with

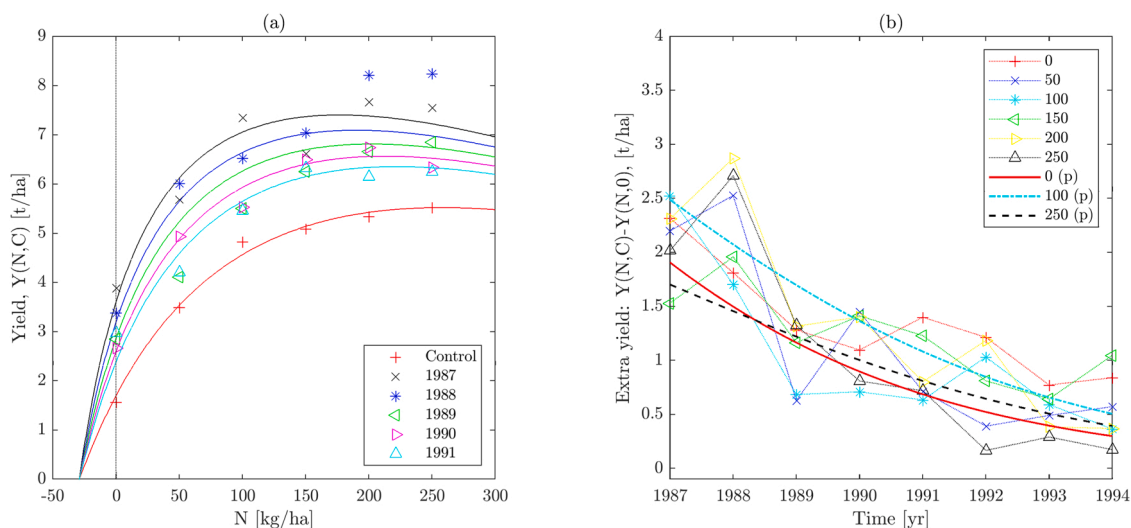


**Fig. 2.** ‘Dynamic fitting’: example of decay of the extra yield following the discontinuation of organic amendments (FYM). Dataset: Winter wheat yield from Woburn Organic Manuring experiment (period: 1987–1994). (a) Yield: the predicted response curves (lines) for the period 1987–1991 are calculated using the reciprocal response curve Eq. (3) combined with the yield-enhancing carbon decay Eq. (6) and the parameter values in Table 1. Legend: 1987 (black), 1988 (blue), 1989 (green), 1990 (magenta), 1991 (cyan), Control: no OM (red); the symbols (+, x, \*, ...) correspond to the observed mean yield. (b) Time dependence of the extra yield  $\Delta$  for different N rates (dotted lines with symbols): the predicted extra yield (smooth lines, p) is given for three nitrogen rates (0, 100, 250 kg N/ha).

modifications and its purpose is to evaluate, from crop yields and soil analyses, the cumulative effects of organic matter on a light, poorly-structured, sandy soil with a long history of arable cropping.

The experimental design is organised around four blocks of eight plots and has had three different phases from 1964 (Macdonald et al., 2019). We make use of data from the second phase spanning the period 1981–1994 (Mattingly et al., 1981–1994). Each plot was split into 6 N treatments. During an initial stage, fertility was built up from several organic amendments, a series of crops being grown sequentially; in the second stage, amendments were ceased.

During the build-up stage (1981–1986) of the second organic manuring phase, the plots in each block received several types of organic amendments with different carbon concentrations: farmyard manure (Fd), wheat straw (St) and clover grass ley (Lc). In each block, four plots had grass ley with clover but were distinguished based on their previous treatment history, having been treated with nitrogen, peat or green manure in the previous experimental design. Finally, two control plots (Fd, Fs) received no organic carbon input, however, being treated with doses of mineral nutrients, without N (i.e. P, K, Mg fertiliser), equivalent to the nutrient content of the farmyard manure (Fd) or straw treatments (Fs). On the plots without any grass ley, crops (barley, bean, wheat, sugar beet, oat, rye) were grown sequentially. In Sec. 2.3.2, 3.1 where the parameters of the response curve are identified, we shall focus on the plots which received farmyard manure (FYM). In this article, we will not try to account for the contribution of crops on the accumulation of soil organic matter during this stage.

In the subsequent cropping stage (1987–1994), organic amendments were discontinued on the plots, which were each split into 6 sub-plots to test five rates of nitrogen fertiliser and nil (0, 50, 100, 150, 200, 250 kgN/ha). In terms of crops, the winter wheat cultivar Mercia was grown (almost) continuously for 8 years over the four blocks. The year 1987 was a hybrid in its experimental design because only two replicates (blocks i, iii) were ploughed for the first test crop (winter wheat), while the other replicates kept the design of the build-up phase with plots of leys and winter oats. For the period 1988–1991, crops alternated in each block between winter wheat and other crops (potato, winter bean) so in each year there were two replicates sown to wheat. This therefore formed a gapless time series of wheat. We are thus neglecting the effects on yield of this rotation of crops with a sub-set of yield data restricted to blocks (i,iii), using blocks (ii,iv) for 1988 and 1990 only. The wheat

yield data from the four blocks are however used for the three final years 1992–1994 as explained below.

### 2.3. Nutrient response curves

To assess the simultaneous response of crops to organic matter and to nitrogen fertiliser a combined response curve is needed. A response curve based on inverse polynomials was tested in the evaluation of yields from experimental plots receiving organic amendments and a range of fertiliser N treatments.

#### 2.3.1. Inverse polynomials

Response curves relate crop yields to levels of applied nutrients such as from fertiliser. Here we follow the semi-empirical theory for fertiliser response developed in Greenwood et al. (1971). This theory proposes that the relation between yield and nutrient supply can be expressed as an inverse polynomial of the form

$$\frac{1}{Y(N, \dots)} = \left[ \frac{1}{A} + \frac{1}{B(N_s + N)} + \dots \right] \left[ \frac{1}{1 - (N_s + N)/\alpha} \right] \quad (2)$$

where  $Y$  represents yield and  $N$  the total amount of applied nitrogen from inorganic fertiliser. The three dots ellipsis refers to possible additional terms related to other nutrients such as phosphorus and potassium, which we disregard in this article. Note however that the developments to follow can be extended easily to these nutrients. The parameters  $A$ ,  $B$  and  $N_s$  represent respectively: the theoretical maximum yield obtainable before adverse effects of excess nitrogen take effect (i.e.  $Y \sim Y(N/N_s \gg 1)$ ), the maximum crop response rate (i.e. the slope of the response curve for no application  $B \sim Y'(N=0)$ ) and the indigenous soil nitrogen prior to fertiliser application. The parameter  $\alpha$  corresponds to a growth inhibitor coefficient associated with the osmotic pressure increase in the root zone determined by the nitrogen level, leading to the response curve downturn commonly observed (Greenwood et al., 1971).

Mechanistically, the parameter  $B$  can be related to the mass flow transport of nitrogen within the soil, which establishes a nitrate concentration gradient decreasing away from the root surface (Greenwood et al., 1971). As soil organic matter and carbon turnover are key to determining soil structure and its ensuing water flow and nutrient transport properties (e.g. Neal et al., 2020), this suggests that  $B$  may vary with the soil carbon content, say  $C$ . Actually, because plants do not use

soil carbon directly, we shall model the yield-enhancing effect of organic amendments with a dimensionless proxy variable, say  $y$ . For simplicity, we assume that amendments modify  $B$  linearly via this proxy variable, i. e.  $B \rightarrow B(1 + y)$ , to consider the bi-variate response curve

$$\frac{1}{Y(N, y)} = \left[ \frac{1}{A} + \frac{1}{B(1 + y)(N_s + N)} \right] \left[ \frac{1}{1 - (N_s + N)/\alpha} \right] \quad (3)$$

Eq. (3) keeps the structure of the response curve (2) and does not need the introduction of an additional parameter at this stage. Note that (2) is recovered when no organic matter is applied, which corresponds to  $y \equiv 0$ . Eq. (3) forms the two-dimensional response curve equation that we use throughout this article. The link between the  $y$  and  $C$  is described in the section below. Alternatives to Eq. (3) are proposed and discussed in B.

Here we are neglecting the effect of additional nutrients provided by the organic amendments. Note that the exogenous nitrogen from FYM applications can only move the response curve horizontally. This is not sufficient for explaining the diagonal shift of the response within the north-west corner of the response ( $N$ ,  $Y$ )-plane (Fig. 2) caused by the organic amendments. We will show that the idea of introducing the carbon proxy variable  $y$  to modify the slope of the response curve at low  $N$  rates suffices to capture the effect of FYM applications. Including nutrients in the amendment, the applied organic  $N$  in particular, is not straightforward and needs considering in terms of the dynamical processes of mineralisation, immobilisation and leaching; we leave this for future work. Yet, in the context of the Woburn experiment, the C/N ratio of the FYM applications was about 15 kg N/kg C, which suggests that significant mineralisation may have occurred during the experimental build-up stage. Because the soil at Woburn is sandy and poorly structured, and because the FYM is applied in the autumn, most of this mineralised organic  $N$  may have been leached during this stage of the experiment and little of this 'applied  $N$ ' remained prior to cultivation during the experimental phase 1–6 years after application. Hence we may hypothesise that this residual nitrogen from FYM (in 1987) is taken into with the native  $N_s$  parameter included in our response curve. Provided that this remains true every season, the validity of our optimal control theory will not be impeded.

### 2.3.2. Parameter identification: a dynamic response accounting for fertility decay

We use the set of yield data of the Woburn Organic Manuring long term experiment when winter wheat was grown continuously over the 1987–1994 period (Sec. 2.2). Over the eight years of data, yields of winter wheat varied greatly from year to year, almost certainly as a result of the different weather in each year. Van der Pauw (1962) demonstrated the relationship between the loss of  $N$  from leaching and reduction in yield in certain crops resulting from winter rainfall, but other factors such as solar radiation, temperature, and disease are also almost certainly responsible for the interannual variability (Addy et al., 2020, 2021; Putelat et al., 2021).

However, we can avoid this difficulty by looking at the time variation of the extra yield gained from the organic matter applications. We define the extra yield  $\Delta$  as the difference between the yield observed from plots which have received some OM treatments in phase 1 and the yield measured from the control plots which have not received any OM amendments. In this way we isolate the change in yield that results from the decline in OM alone, which we can track from assuming that the proxy variable is time dependent  $y_t$ . Here the subscript  $t$  denotes the season number or cultivation year. That is

$$\Delta(N, y_t; t) = Y(N, y_t; t) - Y(N, 0; t). \quad (4)$$

This experiment clearly shows that, during cultivation, the extra yield gained by the OM applications in the first stage of the experiment decreases with time (Fig. 2). This feature may reflect the slow decay of the yield-enhancing soil carbon content. Here we discuss a possible

method to estimate the carbon decay rate from yield data, as well as determining the parameters of the response curve.

Our identification method splits the data into two components. The first component consists of a subset of data which received no organic matter, but distinguishing between six nitrogen doses: the observed yield without applied carbon  $\hat{Y}(N, 0; t)$  of the two control plots (Fd, Fs). As shown below, this component is used against the theoretical yield in Eq. (3) with  $y \equiv 0$ , which in effect will smooth out the interannual variability in our nonlinear regression. The second component corresponds to the observed extra yield data  $\hat{\Delta}$  computed for each year and each  $N$  treatment and the two control plots. These two components are then combined together into a vector  $\hat{F} = [\hat{Y}, \hat{\Delta}]^T$  used in the nonlinear regression procedure below. The symbol  $^T$  denotes the transpose operation. In this paper, we restrict the analysis to OM inputs in the form of FYM only. Fig. 2 presents the means for each  $N$  rate of these two datasets of 261 data points each.

Now, the novelty in our methodology is to account for the time evolution of the soil carbon content which yield responds to in the form of the proxy variable  $y_t$ . We emphasise that this is not necessarily the whole carbon content of the soil, but a component that is active in some way relevant to yield, as we are going to show. This component may reflect the water-holding capacity for soil or the hydraulic conductivity, for example. For simplicity, we assume that the carbon content decays via the proxy variable  $y_t$  according to the simple homogenous linear recurrence equation

$$y_t = \kappa y_{t-1} + v_t, \quad (5)$$

where the decay constant  $\kappa \leq 1$  represents the proportion of carbon that remains active in season  $t$  from the previous season. Note that this proportion also gives the characteristic timescale of this process, which can be estimated from the half-life period defined as  $t_{1/2} = \ln(1/2)/\ln(\kappa)$ . As shown below, the forcing variable  $v_t$  will represent the dimensionless amount of yield-enhancing carbon from organic matter amendments in season  $t$ .

At Woburn, winter wheat was grown each year from 1987 (although on alternating blocks until 1990), while organic matter amendments were stopped in 1986, i.e.  $v_t \equiv 0$ ,  $t \geq 1987$ . As a result, according to (5) we expect the carbon proxy  $y_t$  to decay as

$$y_t = y_{86} \kappa^{t-1986}, \quad (6)$$

$y_{86}$  being the value (to be determined) of the carbon proxy variable resulting from the yield-enhancing carbon accumulated from the first stage of the experiment over 1981–1986.

We substitute this expression into Eq. (4), using expression (3), to fit the extra yield data in combination with 'zero carbon' yield data and identify at once the four response curve parameters  $p = (A, B, N_s, \alpha)$  together with the values  $y_{86}$  and  $\kappa$ . This is numerically performed from defining the vector-valued function

$$F(p, \kappa, y_{86}; t; N) = \begin{bmatrix} Y(p; N, 0) \\ \Delta(p; N, y_{86} \kappa^{t-1986}) \end{bmatrix}, \quad (7)$$

which is used with the R nonlinear least-squares routine NLS against the observational data  $\hat{F}$ . Note that the regression is performed with respect to the nitrogen rates  $N$  seen as independent variables, whilst the seasons  $t$  are being treated as imposed parameters setting the level of decay of the carbon proxy  $y_t$ .

In this article, the link with carbon is achieved from assuming a specific form for  $y_t$  and  $v_t$  such as the ratios

$$y_t \equiv \frac{C_t}{C_s}, \quad v_t \equiv \frac{V_t}{C_s}. \quad (8)$$

Here we explicitly suppose that  $y_t$  and  $v_t$  represent the carbon content of the soil, say  $C_t$ , and the organic amendments, say  $V_t$ , with respect to a



reference value of yield-enhancing carbon  $C_s$ , which needs to be determined from the data as we show in [Sec. 3.1](#).

We emphasise that other interpretations for the proxy variable  $y_t$  could be envisaged if the right motivations to do so would become available. Without any such incentives at hand, we use Ockham's razor to select the simplest reasonable hypothesis. The formal developments to follow will be done with respect to the carbon content  $C_t$ , instead of  $y_t$ , both being related by the change of variable above.

#### 2.4. Static analysis using classical optimisation techniques

In this section, we show how the break-even ratio condition arises naturally from classical optimisation and how it generalises to more than one nutrient.

##### 2.4.1. One-dimensional analysis along nitrogen

It is quite natural to identify the response curve as a production function whose output is the yield  $Y$  as a function of the inorganic nitrogen input  $N$  due to fertiliser applications. Denoting  $p$  and  $c$  the price of the crop and the cost of inorganic fertiliser respectively, the profit is defined by the nonlinear function

$$J(N) = pY(N) - cN. \quad (9)$$

Without any additional constraint to satisfy, the optimum nitrogen input  $N_+$  maximising the profit corresponds to a critical point of  $J(N)$ , which solves  $J'(N_+) = 0$  by definition. We denote with a prime the derivative of a function. Therefore, the unconstrained maximisation of profit leads directly to the BER (break-even ratio) condition

$$Y'(N_+) = c/p, \quad (10)$$

giving the optimum rate of fertiliser application to obtain maximum economic yield. Economists call the derivative  $Y'$  of the production function  $Y$  with respect to the resource variable the 'marginal physical product' ([Samuelson, 1980](#); [Chiang, 1984](#)). Note that we can define the metric

$$\gamma(N) = pY'(N) - c \quad (11)$$

which characterises a distance to optimality as the difference between the crop 'marginal revenue product'  $pY'(N)$  and the fertiliser marginal cost  $c$  (in £/kg N). For conciseness, we will speak of marginal product for terms like  $pY'$  in what follows. As long as  $\gamma > 0$ , the BER condition is not met, and profit could be increased by adding more nitrogen until  $\gamma = 0$ . In Economics, such a quantity is usually interpreted as a 'shadow price', which has the physical dimension of price (or value) per unit of resource (i.e., £/kg N). If we denote  $\delta N$  an increment of nitrogen fertiliser, this price  $\gamma$  multiplied by  $\delta N$  represents exactly the increment in profit  $\delta J$  gained from the ensuing increase in yield  $\delta Y = Y'\delta N$ , i.e.

$$\gamma\delta N = pY'(N)\delta N - c\delta N = p\delta Y - c\delta N = \delta J. \quad (12)$$

In other words,  $\gamma$  indicates how much profit changes whenever the quantity of resource ( $N$ ) available changes by one unit. This is nothing but formalising mathematically the intuitive reasoning behind the BER approach. If  $\gamma < 0$ , the value of the extra yield obtained (i.e., the crop marginal product) is less than the cost of the extra  $N$  (i.e., the fertiliser marginal cost) to grow it; money is being wasted and so profit declines. Maximum profit is reached when both balance, that is  $\gamma = 0$ . This is a well-known condition for maximizing profit in Economics ([Samuelson, 1980](#), p. 508).

##### 2.4.2. Two-dimensional analysis along nitrogen and carbon

The static optimisation of fertiliser application can be generalised to more than one nutrient. Expression (9) remains valid but needs to be interpreted as a function of several variables. Although organic matter is not directly a plant nutrient, a yield response curve can still be deduced

in which yield depends on the carbon content (or amount applied) using inverse polynomials as we showed in the previous section.

To be explicit, the two-dimensional interpretation of (9) reads

$$J(N, C) = pY(N, C) - cN - qC, \quad (13)$$

where  $q$  is the cost of applying organic matter. The unconstrained optimum rates ( $N_*$ ,  $C_*$ ) of inorganic nitrogen and carbon from organic matter amendments then correspond to the critical point of  $J(N, C)$  now solving the system

$$Y_N(N, C) = c/p, \quad Y_C(N, C) = q/p, \quad (14)$$

where we denote  $Y_N = \partial Y/\partial N$  and  $Y_C = \partial Y/\partial C$  the partial derivatives of  $Y$  with respect to  $N$  and  $C$ . We interpret this system of two equations as the two-dimensional BER condition. As in the one-dimensional case, we can define the nitrogen and carbon shadow prices

$$\gamma(N, C) = pY_N(N, C) - c, \quad \eta(N, C) = pY_C(N, C) - q. \quad (15)$$

#### 2.5. Dynamic analysis using optimal control theory

Here we aim at computing the optimal application rates of inorganic nitrogen and organic matter to apply every year over a cultivation period of  $T$  years in order to maximise the overall profit. We follow a nonlinear programming approach to solve the discrete-time optimal control problem defined below.

##### 2.5.1. Formulation

Our formulation relies on the key assumption according to which both the soil nitrogen and carbon evolve in time season after season. Importantly this implies that we need to distinguish the nitrogen and carbon content in the soil,  $N_t$  and  $C_t$  say, from the nitrogen and carbon content in the inputs,  $U_t$  and  $V_t$  say. Note that this distinction is irrelevant in the static analyses developed above. In terms of optimal control, the former set of variables correspond to state variables, while the latter set of variables represents control variables.

Now we need to assume that crops respond to the state rather than control variables, because the former characterises the soil. In this sense, we shall refer to 'field or soil fertility' in this article. More specifically, by fertility, we shall mean the combined effect of both the fertiliser and organic matter applications together with the internal dynamics (gain or loss) of the yield-enhancing nitrogen and carbon in the soil ( $N_b$ ,  $C_b$ ).

In contrast to the static approach, the dynamics between state and control variables must indeed be considered. Modelling the processes governing the (spatio)temporal evolution of the soil nitrogen and carbon is fraught with difficulties and is still a matter of intense research. For the problem at hand, however, some useful insights are gained from treating this multitude of complex processes as simple recurrence equations.

For simplicity we suppose that the dynamics of the soil nitrogen and carbon is linear and uncoupled and that their respective concentrations in season  $t$  result from the sum of a carry-over proportion from the previous season  $t - 1$  with the actual nitrogen input and organic matter amendment in season  $t$ ,  $t \in [1, T]$ . Mathematically this translates into the two recurrence equations

$$N_t = kN_{t-1} + U_t, \quad C_t = \kappa C_{t-1} + V_t. \quad (16)$$

They can be integrated once initial conditions describing the level of pre-existing fertility conditions at  $t = 0$

$$N_0 = N_i, \quad C_0 = C_i, \quad (17)$$

and a sequence of inputs ( $U_t$ ,  $V_t$ ) are known.

The optimal control theory ([Pontryagin, 1987](#); [Intriligator, 1971](#); [Clark, 1976](#); [Sage and White, 1977](#); [Sethi, 2019](#)) is a mathematical optimisation technique which determines the optimal temporal

trajectories (sequence) for the control variables to maximise (or minimise) some objective function,  $J$  say, subject to a set of constraints such as the two recurrence equations above. Here we seek to maximise profit over a finite period of  $T$  years, our objective function being

$$J(N_t, C_t; U_t, V_t) = \sum_{t=1}^T [pY(N_t, C_t) - cU_t - qV_t]. \quad (18)$$

In this article, inflation is disregarded, and no discount factor is introduced for simplicity and because infinite cultivation horizon problems are not considered.

In contrast to the static analysis developed above, we now deal with a discrete-time dynamical system corresponding to a deterministic multistage decision process (Bellman, 2013; Intriligator, 1971; Sage and White, 1977; Sethi, 2019). The time dependence involved by the recurrence equations needs a specific treatment that we explain now.

### 2.5.2. Necessary conditions for optimality

The presence of (time-dependent) constraints in optimisation problems such as Eq. (16) requires variables, called Lagrange multipliers, equal in number to the number of constraints. The Lagrange multipliers ensure that the constraints are satisfied at all times. In broad terms, these multipliers estimate how much the objective function changes due to a unit change in the value of a constraint. That is, in our case, a change in the increment of fertility  $N_t - N_{t-1}$  and  $C_t - C_{t-1}$ . These multipliers generalise the BER concept in the sense that they reflect the change in profit that results from a unit increment of the soil fertility. In economic terms, these multipliers are shadow prices giving a monetary value to the increase (or loss) of fertility. Our analysis thus generalises the BER concept to all aspects of fertility (if the yield response is well-understood) (i) in the current year and (ii) future years (in terms of today's outlook) and for (iii) for multiple inputs.

In contrast to the unconstrained static optimisation (Sec. 2.4), it is not simply the objective function that needs to be differentiated with respect to the variables but the so-called Lagrangian function,  $L$  say. Such a function is defined as a linear combination of the objective function and the constraints, which reads in our case

$$L = \sum_{t=1}^T \{ [pY(N_t, C_t) - cU_t - qV_t] + \lambda_t (kN_{t-1} + U_t - N_t) + \mu_t (\kappa C_{t-1} + V_t - C_t) \} + \lambda_0 (N_t - N_0) + \mu_0 (C_t - C_0) + \sum_{t=0}^T (\nu_t N_t + v_t C_t) + \sum_{t=1}^T (\zeta_t U_t + \xi_t V_t). \quad (19)$$

We denote  $\lambda_t$  and  $\mu_t$  the Lagrange multipliers associated with the two recurrence equations governing the dynamics of nitrogen and carbon respectively (the multipliers associated with the initial conditions are denoted  $\lambda_0$  and  $\mu_0$ ). The variables  $\nu_t, v_t, \zeta_t, \xi_t$  are Lagrange multipliers needed to ensure that  $N_t, C_t, U_t, V_t$  are all non-negative quantities. We will see later that  $\zeta_t$  becomes key to the analysis once organic amendments stop. Note that all these multipliers are time dependent necessarily. Hence, one of the first tasks is to determine their equations of evolution. This is object of optimal control theory.

Without entering into the mathematical details, taking the partial derivatives of  $L$  with respect to the state variables ( $N_t, C_t$ ) leads to the recurrence equations that we are seeking,

$$k \lambda_{t+1} = \lambda_t - pY_N(N_t, C_t) - \nu_t, \quad \kappa \mu_{t+1} = \mu_t - pY_C(N_t, C_t) - v_t. \quad (20)$$

A similar calculation at the initial and terminal times,  $T$ , gives the associated boundary conditions

$$\lambda_T = pY_N(N_T, C_T) + \nu_T, \quad \mu_T = pY_C(N_T, C_T) + v_T, \quad (21)$$

and

$$\lambda_0 - \nu_0 = k\lambda_1, \quad \mu_0 - v_0 = \kappa\mu_1. \quad (22)$$

Eqs. (20) and (21) suggest  $\lambda_t$  and  $\mu_t$  should be interpreted as the shadow

prices of nitrogen and carbon whose evolution is determined by comparison to the respective marginal products of fertility. They provide us with the price of the marginal (extra) value gained from the increase in yield generated by an increment in fertility, in terms of either nitrogen or carbon contents. The derivatives with respect to the control variables (i.e., the inputs) yield two important relations, namely

$$\lambda_t = c - \zeta_t, \quad \mu_t = q - \xi_t. \quad (23)$$

Finally, we have the complementary slackness conditions (Sethi, 2019)

$$\begin{aligned} \nu_t \geq 0, \quad \nu_t N_t = 0; \quad v_t \geq 0, \quad v_t C_t = 0; \\ \zeta_t \geq 0, \quad \zeta_t U_t = 0; \quad \xi_t \geq 0, \quad \xi_t V_t = 0, \end{aligned} \quad (24)$$

which close the system of equations governing the optimal trajectory that one must follow to maximise profit over  $T$  seasons.

The Lagrange multipliers  $\zeta_t, \xi_t$  are of a particular interest. For each season  $t$ , conditions (24) imply that these multipliers are zero if the control variables are strictly positive. In the next section, we will see that this is important as this shows that  $\lambda_t$  and  $\mu_t$  are constants equal to the costs of fertiliser and organic matter amendments as long as the input rates are non-zero ( $U_t > 0, V_t > 0$  implies  $\zeta_t = \xi_t = 0$ ). This means that a dynamic BER is reached in such a case for season  $t$ . Alternatively, if these Lagrange multipliers (e.g.,  $\xi_t > 0$ ) become non-zero, the inputs must cease (e.g.,  $V_t = 0$ ). One then understands that relations (23), expressed as  $-\zeta_t = \lambda_t - c$  and  $-\xi_t = \mu_t - q$ , represent the dynamic version of the static metrics  $\gamma$  and  $\eta$  in Eq. (15) (Sec. 2.4.2). In other words, inputs must be stopped when their marginal cost (e.g.  $q$ ) exceeds the fertility shadow price (e.g.,  $\mu_t < q$ ). This is very reminiscent of the classical BER approach advocated in the AHDB guidance RB209, (2022). We interpret  $\zeta_t$  and  $\xi_t$  as the shadow prices of fertility loss in terms of nitrogen and carbon, respectively. A similar reasoning stands for  $\nu_t, v_t$ , but is less crucial in this paper. They represent the marginal products of fertility when the soil is depleted in nitrogen or carbon.

Finally, we remark that it is a specificity of the optimal control theory to show that optimal trajectories are actually not only determined by the initial conditions but also by a set of terminal conditions, whose importance is clearly demonstrated in the subsequent sections. This leads to a so-called two-point boundary value problem, bounding the system state between two instants in time. For discrete-time problems, however, it is more effective to turn this around by reformulating this approach in terms of nonlinear programming. It makes the numerical solution of the above equations also more amenable in practice.

### 2.6. Computation of an optimal trajectory

The optimal trajectory leading to optimal inputs maximising profit solves the nonlinear dynamical system formed by the recurrence Eqs. (16) and (20) associated with the boundary conditions (17) and (21), subjected to the additional conditions (22)–(24).

This nonlinear system has the steady-state ( $N^*, C^*, U^*, V^*, \lambda^*, \mu^*$ ), which is obtained from solving

$$(1-k)c = pY_N(N^*, C^*), \quad (1-\kappa)q = pY_C(N^*, C^*), \quad \lambda^* = c, \quad \mu^* = q. \quad (25)$$

We call this the dynamic BER equilibrium. The associated values of the inputs ( $U^*, V^*$ ) follow from the solution of the linear system (16) with  $(N_t, C_t) = (N^*, C^*)$  for all  $t$ , given by

$$U^* = (1-k)N^*, \quad V^* = (1-\kappa)C^*. \quad (26)$$

Because we allow fertility to build up with time, these two equations show that the nitrogen and carbon inputs each year can be reduced, compared to what would be expected from the static BER analysis. Note that the steady-state ( $N^*, C^*, U^*, V^*$ ) represents the optimal control solution of our problem for the infinite horizon case  $T \rightarrow \infty$ .

We emphasise that these formulae are reminiscent of equations (14)

**Table 1**

Parameter values of the inverse polynomial response curve (3) using the Woburn organic manuring long term experiment. See Sec. 2.3.2 for the identification method and Fig. 2.

Parameters	A	B	$N_s$	$\alpha$	$\kappa$	$y_{86}$	$\nu$	$C_s$	$C_{86}$
Units	t/ha	t/kg N	kg N/ha	kg N/ha	—	—	—	t C/ha	t C/ha
Values	12.2	0.0705	29.3	1050	0.748	2.14	0.654	5.95	12.7

from the two-dimensional static analysis in Sec. 2.4.2 but clearly modified by the decay constants. This is not a surprise as the dynamics of nonlinear dynamical systems tend to be controlled by attractors such as equilibria. In the numerical results presented later, we will see that this steady-state is very important as it governs the levels of soil fertility and inputs along any optimal trajectory until a critical season at  $t = t_*$  years from which the organic amendments must be reduced and then stopped if maximum profit is to be obtained.

Note finally that this steady-state is characterised by Lagrange multipliers whose values are set by the cost of inputs, i.e.  $(\lambda_*, \mu_*) = (c, q)$  (Sec. 2.5.2). Here we see a clear example of the interpretation given to the Lagrange multipliers as shadow prices. Once the steady-state is reached, they must equal the cost of the inputs, as is the case with the classical BER concept for nitrogen.

For the full computation of an optimal trajectory, as we hinted in the previous section, we found that it is numerically much easier to reformulate our discrete-time optimisation problem as the search of a constrained minimum of a function of several variables as is done in nonlinear programming (Mangasarian, 1969; Sage and White, 1977). We then need simply to minimise  $-J$  defined as a scalar function of an unknown vector, say  $\mathbf{z}$ , whose components are made of the state and control variables of every season. Specifically, we defined  $\mathbf{z} = [N_0, C_0, \dots, N_T, C_T, \dots, N_T, C_T, U_1, V_1, \dots, U_T, V_T, \dots, U_T, V_T]^T$ , where the symbol  $^T$  denotes the transpose operation.<sup>fn1</sup> Numerical solution can be obtained from using a constrained optimisation routine such as the MATLAB FMINCON routine, for which the objective function is given by the T-year profit function (18) subject to the (linear) constraints represented by the nitrogen and carbon dynamics (16) with initial conditions (17), imposing the inequality constraints  $\mathbf{z} \geq 0$ . Analytically, the necessary conditions for optimality (Sec. 2.5.2) are derived within this framework from Kuhn-Tucker's conditions (Mangasarian, 1969; Sage and White, 1977).

### 3. Results

#### 3.1. Response curve parameter identification

In this article, we focus on FYM amendments, leaving the study of the other organic treatments (straw, leys) to future work. The results of fitting the inverse polynomial response curve described in Sec. 2.3.1 are presented in Table 1. Regarding the carbon proxy dynamics, we found

$$\kappa = 0.748, \quad y_{86} = 2.14. \quad (27)$$

The value of  $\kappa$  gives  $t_{1/2} = 2.39$  years. A word of caution though. Given that the data are variable to within one tonne or so, some values of the mean extra yield are likely to be negative if on average the expected value of the extra yield becomes small but it would lead to error in the estimates of  $\kappa$  and  $y_{86}$  if we excluded these data. For the Woburn dataset of interest, over the 261 extra yield estimates  $\Delta$  (Eq. (4)), 49 of these were negative and occurred at all nitrogen treatments. Fig. 2(b) shows however that the mean extra yield is well-behaved (i.e.  $\geq 0$ ) despite sawtooth fluctuations, whose understanding is left for future work. A less noisy dataset, with access to four replicates of data for the whole period

<sup>1</sup> The  $4T + 2$  components of  $\mathbf{z}$  are thus related to the state and control variables by  $N_t \equiv \mathbf{z}_{2t+1}$ ,  $C_t \equiv \mathbf{z}_{2t+2}$ ,  $U_t \equiv \mathbf{z}_{2(T+1)+2t-1}$ , and  $V_t \equiv \mathbf{z}_{2(T+1)+2t}$  for  $t \in [1, T]$ .

of interest in particular, would increase the precision of our methodology.

Despite this, we think that our identification method has the great advantage to allow the determination of a single set of parameters for the response curve, valid for a wide range of nitrogen and organic matter application rates. Besides, the power of using a proxy variable is to recognise that the processes driving the yield-enhancing property of organic amendments remain unclear and takes advantage of the abstraction that mathematics can bring to this knowledge gap. Nevertheless, our method and formalism pave the way for integrating carbon dynamics or any other driver into the response of crops to inputs.

As explained in Sec. 2.3.2, the proxy variable  $y_t$  is assumed to be a dimensionless metric of soil carbon relying on the reference value of yield-enhancing carbon  $C_s$ , which we identify using first stage of the Woburn experiment of interest. For simplicity, we make the drastic assumption that the carbon inputs from FYM amendments were constant over the 1981–1986 period. That is  $\nu_t \equiv \nu$ ,  $V_t \equiv V$  for  $1981 \leq t \leq 1986$ . It follows that the analytical solution of (5) reads

$$y_t = \frac{1 - \kappa^{t-1980}}{1 - \kappa} \nu, \quad 1981 \leq t \leq 1986. \quad (28)$$

In 1986, we then have  $y_{86} = \nu(1 - \kappa^6)/(1 - \kappa)$ , which yields an estimate of  $\nu = 0.654$  from the values of  $\kappa$  and  $y_{86}$  identified above (Table 1). The yield-enhancing carbon of reference  $C_s = V/\nu$  is calculated from the organic amendments carbon content  $V$ , which can be measured from OM chemical analysis. In the experiment, the rate of fresh matter application of FYM was indeed constant equal to 50 t/ha every year in stage 1. The mean measured percentage of dry matter (% DM) was 24.3%, which then corresponds to an average rate of 12.2 t/ha of applied dry matter each year. The averaged value of carbon input from FYM amendments amounts for  $V = 3.89$  t C/ha, assuming a typical value of 32% of dry matter for the carbon content (Ekland and Kirchmann, 2000; Powlson et al., 2012). Hence, we have  $C_s = 5.95$  t C/ha, which yields  $C_{86} = 12.7$  t C/ha.

The parameter values that we find using this two-step identification procedure are all collected in Table 1. Fig. 2 shows that our procedure predicts well, on average, the reduction in yield associated with the yield-enhancing carbon decay. The statistical details of the fitting performance are reported in B and can be compared with the 'lexp' response curve. Both the reciprocal and 'lexp' response curves give good fitting results. The study (not presented here) of the residuals showed that they are normally distributed with an acceptable homogeneity of variance. However, the reciprocal model minimises the value of Akaike's Information Criterion (AIC) (Burnham and Anderson, 2002) and hence is selected (see B) for the application of the optimal control theory developed in Sec. 2.5.

#### 3.2. Optimal trajectories and input rates

Unless otherwise stated, the numerical results presented in Sec. 3.2 are performed with the reciprocal response curve (3),(8) whose parameters (Table 1) are identified with the methodology described in Sec. 2.3.2 and 3.1. We recall that the rate of loss of yield enhancement due to organic amendments is  $\kappa = 0.748$  in this instance. Based on previous observations (Addiscott and Whitmore, 1987; Bradbury et al., 1993), we set the decay rate of nitrogen arbitrarily to  $k = 0.15$  ( $t_{1/2} = 0.37$  yr), mimicking the observed rapid loss of mobile nitrogen.

According to Beattie (2020), we use typical orders of magnitude for

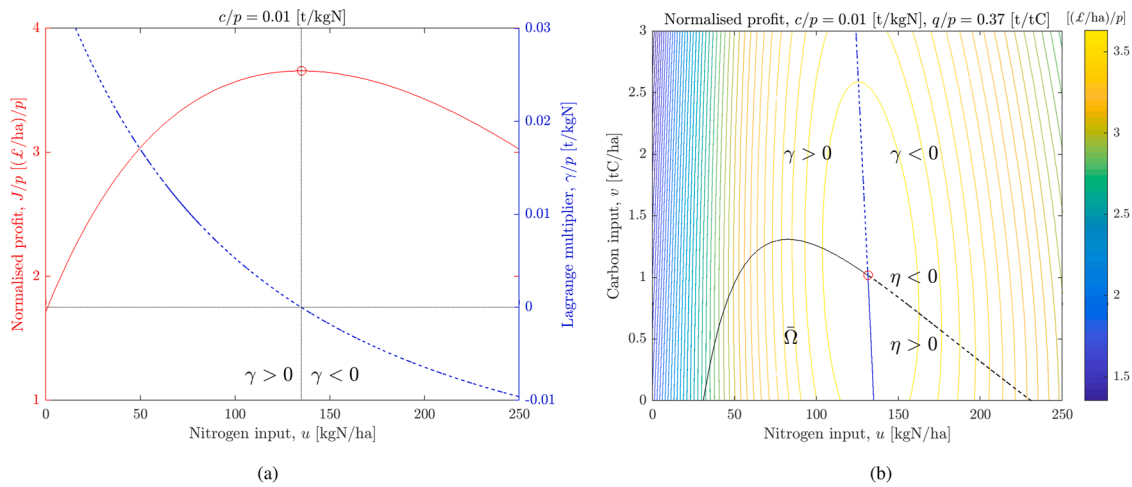


**Fig. 3.** (a) One-dimensional static profit analysis calculated for the OM free yield response  $Y(N, 0)$ . Left hand axis and red line plot the increase in profit expected with applied  $N$  (lower horizontal axis). Right hand axis and blue line display the change in Lagrange multiplier with normalised cost:price ratio (top horizontal axis) and (b) two-dimensional static profit maximisation. Axes plot rate of carbon applied ( $v$ , vertical axis) against amount of  $N$  applied ( $u$ , horizontal axis). Lines give the rates of  $C$  and  $N$  applied that are consistent with optimum rate of application of  $C$  (black) or  $N$  (blue), see Eq. (15). This divides the plotted area into 4 sections. It is only where both Lagrange multipliers ( $\gamma, \eta$ )  $> 0$  that it is profitable to increase applications (region  $\bar{\Omega}$ ).

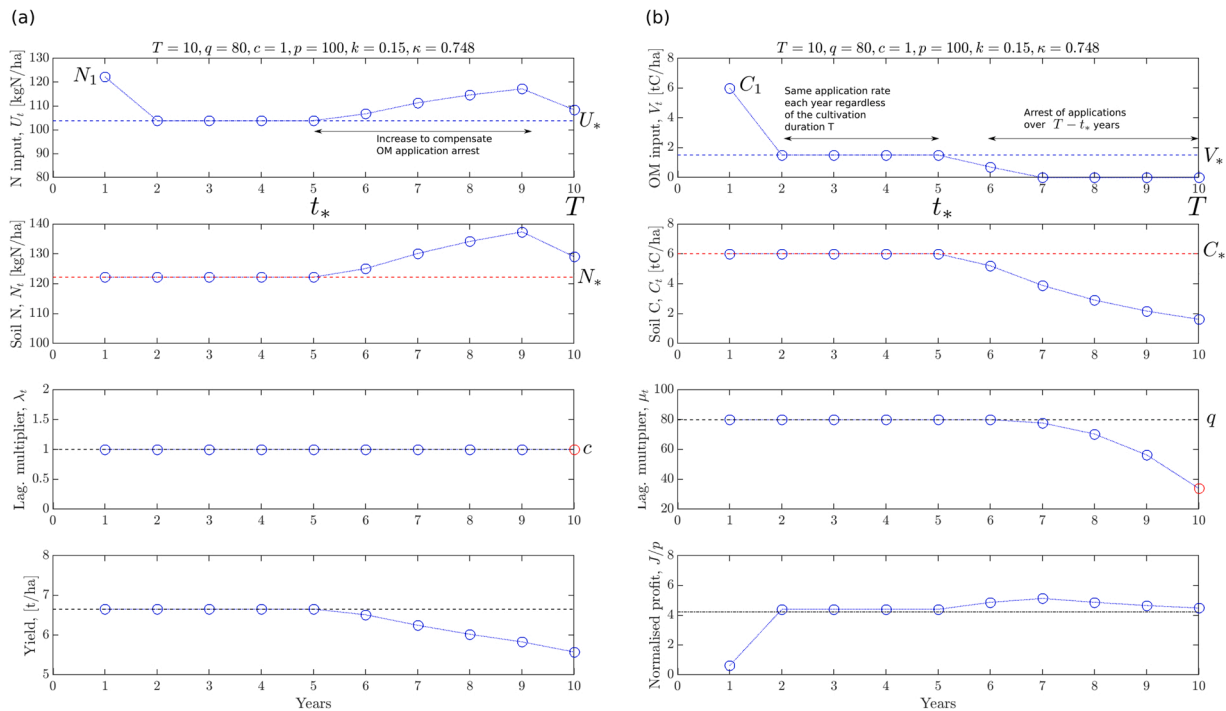


**Fig. 4.** (a) Nitrogen and (b) carbon optimal trajectory for  $C_0 = 0$  t C/ha. The time schedule for nitrogen and carbon amendments divides into three successive portions. First, the inputs in season 1 ( $N_1, C_1$ ) = ( $N^*, C^*$ ) compensate for the initial depleted fertility so that the second phase corresponds to the dynamic BER equilibrium. The third and final phase is associated with the reduction and arrest of organic amendments over three years. This discontinuation in carbon inputs is associated with a slight decrease in yield; however, profit is still maximised over  $T$  years of cultivation. Parameter values:  $T = 10$  yr,  $q = 80$  £ /t C,  $c = 1$  £ /kg N,  $p = 100$  £ /t,  $k = 0.15$ ,  $\kappa = 0.748$ ,  $N_0 = C_0 = 0$ .

the crop price, the cost of nitrogen and organic matter set to  $p = 100$  £ /t,  $c = 1$  £ /kg N,  $q = 80$  £ /t C. Note that the profit functions (13), (18) can be normalised with respect to the crop price  $p$ . In turn all our numerical calculations remain valid for costs of inputs such that  $c/p = 0.01$  t/kg N and  $q/p = 0.8$  t/t C.

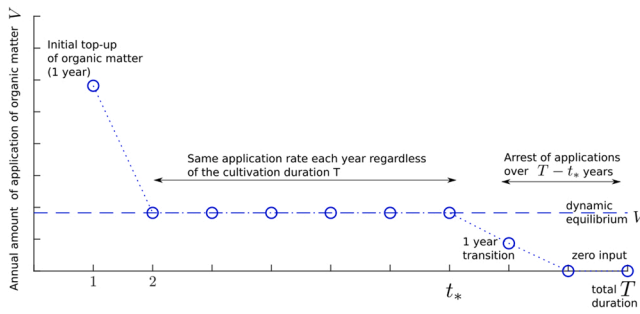
3.2.1. Static analysis

Fig. 3 illustrates the calculations and concepts presented in Sec. 2.4. In the one-dimensional case (Sec. 2.4.1), solving Eq. (10) for the

parameter values listed Table 1 yields the 1D BER nitrogen rate  $N_+ = 135$  kg N/ha for the case of no organic amendment ( $\gamma = 0$ ).<sup>fn2</sup> The corresponding maximum of profit is  $J = 366$  £ /ha. In Fig. 3(a), the locus of the one-dimensional BER optimum is highlighted with a (red) circle symbol. We point out that this  $N_+$  rate corresponds by definition to the

<sup>2</sup> This value is closed to a BER rate of 140 kg N/ha recommended in the AHDB guidance RB209 for light sandy soils subject to moderate annual rainfall.





**Fig. 5.** Typical optimal organic matter amendments schedule. Over a cultivation period of  $T$  years, organic matter amendments follow a three-step timetable. After an initial input in year 1 whose level depends on the concentration of active carbon  $C_0$  prior to the start of the cultivation period, organic matter is applied at a constant dynamic BER rate  $V_*$  (i.e. see dynamic equilibrium Eqs. (25)–(26)) for  $t_* - 1$  consecutive years. Applications are then reduced and stopped over a final phase of  $T - t_*$  years.

can generate more profit. This is the domain  $\bar{\Omega}$  in Fig. 3(b) in which both the shadow prices  $\gamma$  and  $\eta$  are non-negative. Outside this region, applying fertiliser and organic matter becomes too costly with respect to the ensuing yield increase. Note that, if one were limited in the amount of organic amendment, the optimum rates would be given by the solid blue line (Fig. 3(b)). If one were limited in terms of nitrogen, the solid black line would give the optimum rates to apply.

We remark that such a profit landscape is only possible provided that the cost of organic matter  $q$  is low enough. That is why, in Fig. 3(b), computations are done with  $q = 37 \text{ £/t C}$ , which is the cost of OM application that corresponds to a trailerful (12 t/ha of fresh matter) of FYM to reach the carbon BER rate  $C_\times$ . When the cost of OM is too expensive and above a critical value of  $q_c = 43.2 \text{ £/t C}$ , there is no carbon BER rate (i.e.  $C_\times < 0$ ).<sup>fn3</sup> In other words, the BER point (red circle) crosses the carbon input axis ( $v = 0$ ) in Fig. 3, which means that organic amendments have become uneconomical in this static view of the problem.

Finally, note that this analysis combining nitrogen and organic

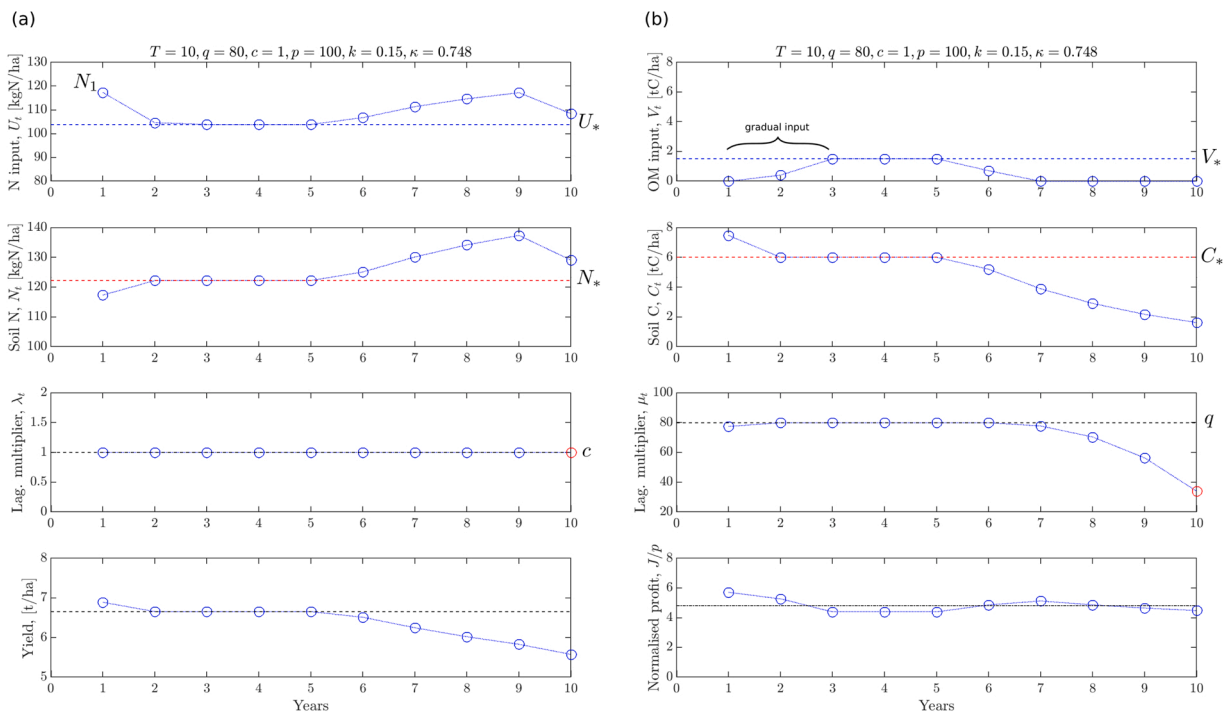


**Fig. 6.** (a) Nitrogen and (b) carbon optimal trajectory for  $C_0 = 10 \text{ t C/ha}$ . In contrast with Fig. 4, the initial high level of yield enhancing carbon  $C_0$  allows a gradual input of carbon over the first three years. The rest of the optimal trajectory is like Fig. 4. Parameter values:  $T = 10 \text{ yr}$ ,  $q = 80 \text{ £/t C}$ ,  $c = 1 \text{ £/kg N}$ ,  $p = 100 \text{ £/t}$ ,  $k = 0.15$ ,  $\kappa = 0.748$ .

rate at which the 1D nitrogen shadow price  $\gamma = 0$ . A decreasing shadow price  $\gamma$  (blue dashed line) for the domain of profitability  $N < N_+$  is of course associated with increasing profit (red solid line).

These features readily translate to the two-dimensional case (Sec. 2.4.2, Fig. 3(b)). The landscape of profit is still concave but now looks like a hill with a relatively flat summit located at the 2D BER rates  $N_\times = 131 \text{ kN/ha}$  and  $C_\times = 1.02 \text{ tC/ha}$ ;  $J_\times := J(N_\times, C_\times) = 369 \text{ £/ha}$  (red circle). Note that for an N application rate 20% below this optimum, profit is only reduced by about 1.3%. In Fig. 3(b), we use an iso-contour plot to show the variation in profit with changing nitrogen and carbon inputs. Such a landscape is structured around the two curves defined implicitly by expressions (17). The first curve (blue) is designated as the  $N$ -line where  $\gamma(N, C) = 0$ ; the second curve (black) as the  $C$ -line where  $\eta(N, C) = 0$ . They intersect at the two-dimensional BER point (red circle). As in the one-dimensional case, only a limited domain of the  $(N, C)$ -input plane is profitable in the sense that an increase in the input rates

matter clearly suggests that nitrogen rates can be reduced thanks to organic amendments (blue line Fig. 3(b)). In the static analysis, this shift is modest. The gains in profit are also not very significant. We will see in Sec. 3.2.2 that these conclusions are misleading because the dynamics of nitrogen and carbon has been disregarded.

### 3.2.2. Dynamic analysis

**3.2.2.1. Description of typical optimal trajectories.** We present two typical optimal trajectories computed with the MATLAB routine FMINCON to maximise total profit over a 10-year period, but which differ from their initial yield-enhancing carbon content  $C_0$ . In both cases, we take the

<sup>3</sup> The critical cost is given by  $q_c = pY_C(N_\times^0, 0)$  where  $N_\times^0$  solves  $Y_N(N_\times^0, 0) = c/p$ .

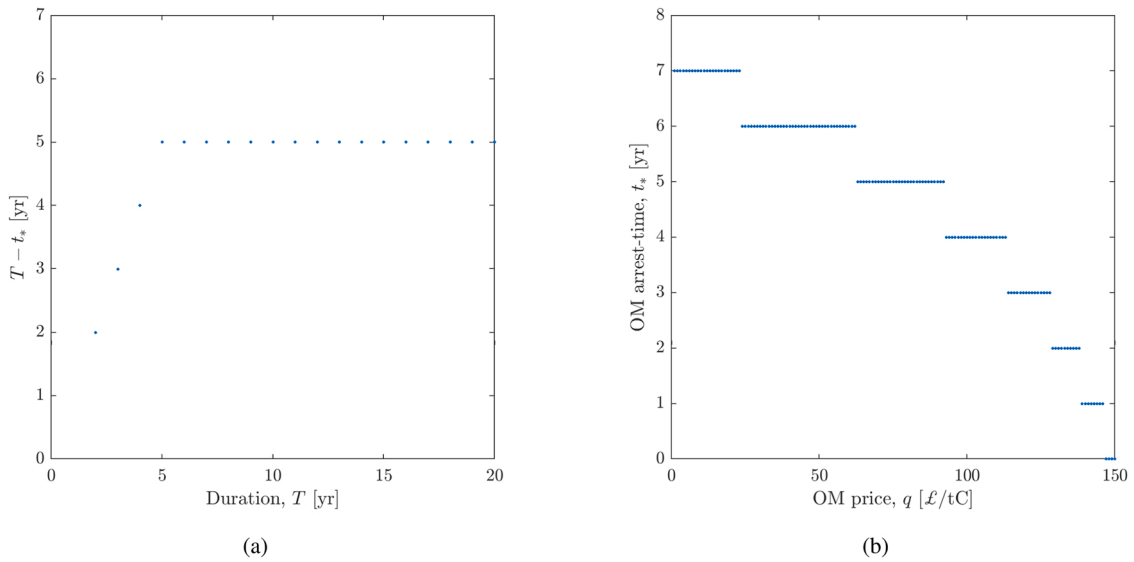


**Fig. 7.** (a) Effect of the cultivation period  $T$  for an OM price  $q = 80$  £ /tC on the OM free period  $T - t_*$ . (b) Effect of the OM price for  $T = 10$  years on the OM discontinuation time  $t_*$ . Note the stepwise decreasing nature of the relation  $t_*(q)$ : the more expensive is the OM, the less is applied. Parameter values:  $c = 1$  £ /kg N,  $p = 100$  £ /t,  $k = 0.15$ ,  $\kappa = 0.748$ ,  $N_0 = C_0 = 0$ .

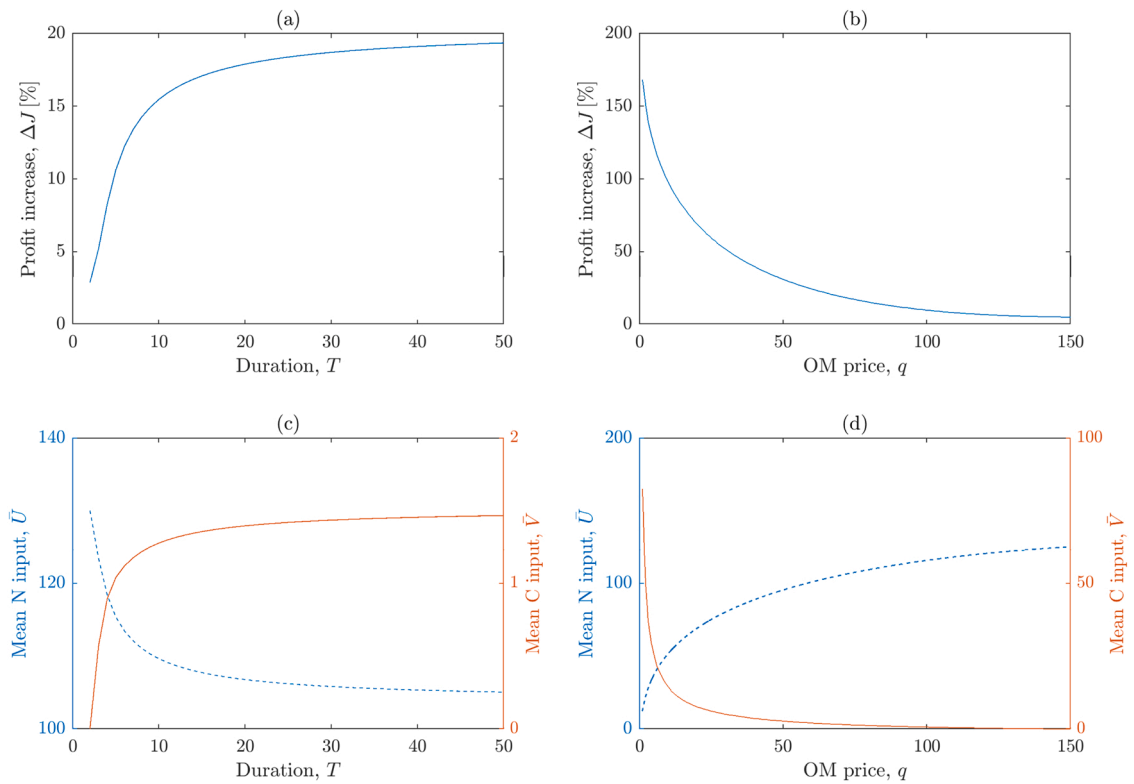


**Fig. 8.** (Left, a,c) Effect of the cultivation period  $T$  for an OM price  $q = 80$  £ /t C. (Right, b, d) Effect of the OM price for  $T = 10$  years. Note the diminishing returns in profit as cultivation period increases. The effect of  $q$  is the reverse because the more expensive is the OM, the less is applied, which in turn reduces profit. Parameter values:  $c = 1$  £ /kg N,  $p = 100$  £ /t,  $k = 0.15$ ,  $\kappa = 0.748$ ,  $N_0 = C_0 = 0$ .

initial nitrogen  $N_0 = 0$  so as to consider the extreme but reasonably realistic case of a degraded soil depleted in nutrients, since even fertile soils may lose much  $N$  during a winter and before applications of fertilizer in spring.

We start with the worst-case scenario where  $N_0 = C_0 = 0$ , Fig. 4 Because of these initial conditions, the trajectory starts at

$$(N_1, C_1, U_1, V_1) = (N_*, C_*, N_*, C_*). \tag{29}$$

Interestingly, we see that the initial depletion can be compensated by the second season if we provide the soil with inputs equal to the dynamic equilibrium  $(N_*, C_*)$  defined by Eq. (25). From year two already, the nitrogen inputs and organic amendments can then drop to their equilibrium values  $(U_*, V_*)$  given by Eq. (26). In turn the soil nitrogen and carbon remain at their dynamic BER values until reaching year  $t_* = 5$ . Fig. 5 presents a generic and schematic schedule for organic matter

applications under the optimal control theory developed in Sec. 2.5.

For the case with a higher level of initial yield enhancing carbon  $C_0 = 10$  t C/ha (Fig. 6), the nitrogen behaves in a similar way because the initial level of nitrogen is the same in both cases. This results from our formulation in which the recurrence equations for the dynamics of nitrogen and carbon are uncoupled. However, the behaviour for carbon is very different initially. Because  $C_0$  is large ( $C_0 > C^*$ ), the optimal trajectory requires a gradual input of carbon over 3 years, starting from none. From the third year,  $U_t = U^*$ . This initial behaviour is a direct consequence of the slow decay of the active carbon, reminiscent of the Woburn data we have described in Sec. 2.3.2, 3.1.

After a short period, dependent on the initial conditions as we just saw, the optimal trajectory tends to the equilibrium point of our system, Eqs. (25)–(26). This dynamic equilibrium is characterised by the soil nitrogen and carbon levels and associated dynamic BER rates  $N^* = 122$  kg N/ha,  $C^* = 6.01$  t C/ha,  $U^* = 104$  kg N/ha,  $V^* = 1.52$  t C/ha for these two examples. Over the 10-year period, the mean nitrogen inputs and organic amendments are  $\bar{U} = 110$  kg N/ha and  $\bar{V} = 1.28$  t C/ha (resp.  $\bar{U} = 109$  kg N/ha,  $\bar{V} = 0.568$  t C/ha) in the first case  $C_0 = 0$  t C/ha (resp. second case  $C_0 = 10$  t C/ha). Note that the nitrogen input values contrast strongly with those calculated under the static two-dimensional analysis ( $N_\times = 131$  kg N/ha,  $C_\times = 1.02$  t C/ha), even for a high cost of organic matter. We see that adding organic matter following optimal trajectories can then lead to both a significant reduction in nitrogen inputs  $\bar{U}$  of about 19% and an increase in (average annual) profit of about 15% (or more if  $C_0 > 0$ ) compared to the BER recommendation used in nitrogen fertiliser guidance ( $N_+ = 135$  kg N/ha) (Fig. 8(a)). We expect these gains to increase with the reduction in the cost of application of organic amendments. This conclusion differs sharply from that in the static analysis case (Sec. 3.2.1.).

These two examples clearly show that the dynamics of the optimal trajectory may differ initially depending on the state of the soil prior to cultivation. But both tend to the dynamic equilibrium of the system very quickly. Hence the memory of the soil initial state is rapidly forgotten along these optimal trajectories once the dynamic equilibrium is reached (in our simple description). As a result, the optimal trajectories evolve identically in time during the final years: here for the final  $T - t^* = 5$  years. From the sixth season, the nitrogen inputs increase to partly compensate, whilst the organic amendments decrease, reaching zero for the final four years.

We can understand the organic matter application schedule from the dynamics of the Lagrange multipliers  $\mu_t$  and  $\xi_t$  determined by Eqs. (20) and (23), which we prefer to write here as

$$\mu_{t+1} - \mu_t = (1 - \kappa)\mu_{t+1} - pY_C(N_t, C_t), \quad -\xi_t = \mu_t - q. \quad (30)$$

The left-hand side equation represents the rate of depreciation of field fertility associated with its degradation. The right-hand side equation corresponds to the loss in marginal profit for the system not to operate along the dynamic BER, i.e., deviate from equilibrium. The fact that there exists a discontinuation time  $t^*$  of OM amendments along an optimal trajectory is caused by the boundary condition (21),  $\mu_T = pY_C(N_T, C_T)$ . Numerically, we find that  $\mu_T < q$ , which implies that OM inputs must be discontinued (Sec. 2.5.2). During this second phase ( $t^* < t \leq T$ ), the marginal product of carbon decays ( $\mu_{t+1} < \mu_t$ ). Interpreting  $(1 - \kappa)\mu_{t+1}$  as the effective marginal cost of the loss in yield-enhancing carbon, we see that the optimal trajectory keeps this cost less than the actual marginal product of fertility  $pY_C(N_t, C_t)$  from one season to the next.

In conclusion, when an optimal trajectory is followed, the equation above must be satisfied at all times, as well as the end boundary conditions Eq. (21). This means that the level of organic matter amendment must be adjusted to avoid wastage. One can see the dynamics of an optimal trajectory as a sequence of quasi-static two-dimensional BER as we have described in Sec. 2.4.2. However, the numerical values of inputs must be adapted to their equilibrium values governed by Eq. (25) in Sec.

2.6 and the decay constants involved in the recurrence equations (16). Note finally that, when organic matter amendments stop, a drop in yield is observed. We then attribute the increase in nitrogen inputs over the 5 final years as a way to compensate this yield loss, which would be more pronounced otherwise.

### 3.2.2.2. Effects of the cultivation period and organic matter price ( $T, q$ ).

Numerical simulations for different  $T$  and  $q$  showed that the time to discontinue organic amendments is  $T - t^* = 5$  years before the end of the cultivation period, taking into account the transition year  $t^* + 1$  of reduced organic amendments before ceasing application. This is a general feature for a range of organic matter application prices, Fig. 7. For the parameter values in Table 1, we found

$$63 \leq q \leq 92 \text{ [£/tC]}. \quad (31)$$

Fig. 7 shows that the relation of the discontinuation time  $t^*$  with  $q$  is a decreasing step function: e.g. when organic amendments are more expensive  $q > 92$  £/tC applications must be stopped one year sooner. Conversely if amendments are cheaper ( $q < 63$  £/t C) they can be applied one more year. Given the current range of price of organic matter applications, we can take the stop time for organic applications as the final six years as a rather general rule for the  $\kappa$  value identified from the Woburn dataset, that is for soils with similar properties and environmental conditions. Note that, short cultivation horizons such that  $T \leq 5$ , i.e. implying  $t^* \equiv 0$ , organic amendments are localised in the first season only. Thus,  $T - t^*$  is the characteristic timescale over which economic benefits of organic amendment can be expected for a given cost of application  $q$  and a specific (yield-enhancing) carbon turnover rate,  $\kappa$ . Essentially where OM is relatively inexpensive the economic benefits accrue over a longer time frame than can be collected because the horizon is so short.

Our numerical calculations also show that the rate of organic matter application in the sixth year before last must be reduced, i.e.  $0 \leq V_{T-t^*-1}$ . This result, combined with the carbon recurrence equation (14.2) with  $V_{T-t^*} = \dots = V_{T-1} = V_T = 0$ , implies that the final season yield-enhancing carbon level  $C_T$  cannot exceed a given proportion of its dynamic BER equilibrium counterpart  $C^*$  set by the decay rate  $\kappa$ , as defined in Sec. 2.5, Eqs. (25)–(26). Calculation shows that we have

$$\kappa^n \leq C_T/C^* \leq \kappa^{n-1}, \quad (32)$$

where  $n - 1$  is the number of seasons with no organic matter application,  $n = T - t^*$ . It should not be a surprise as this arises from the geometric (exponential) decay ensured by (20)<sub>b</sub>.

Numerically, for the decay rates of the yield-enhancing carbon that we expect,  $\kappa \sim 0.75$ , the terminal fertility due to organic matter amendments is then bounded according to

$$24\% \leq C_T/C^* \leq 32\%. \quad (33)$$

This is a rather stark condition, which states that fertility, in Woburn, cannot be maintained beyond a third of what could be accumulated ( $C^*$ ) from continuous amendments. This loss in fertility illustrates the important role of the internal dynamics of carbon and the economics of this problem, both governing the dynamic equilibrium of carbon  $C^*$  determined in Sec. 2.5 by Eq. (25).

Fig. 8 shows the percentage increase in the (10-year) average profit  $\bar{J}$  relative to the (zero carbon) BER profit  $J_+$ , denoted  $\Delta J = 100(\bar{J}/J_+ - 1)$ , and the average rates of nitrogen and carbon inputs ( $\bar{U}, \bar{V}$ ) as  $T$  or  $q$  are varied. We note diminishing returns in profit as the cultivation horizon  $T$  increases. For cultivation horizons from 5 to 15 years, say, organic amendments can generate about 5–15% increase in profit compared the classical (1D) BER recommendation. Similar rapid variations for horizons  $T \leq 15$  years can be seen in terms of inputs (Fig. 8(c)). This suggests that a modest amount of amendments about 1 t C/ha can result in significant savings (> 10%) in terms of artificial fertiliser with

significant economic benefits. The effect of  $q$  is the reverse because the more expensive is the OM, the less is applied, which in turn reduces profit and requires more inorganic fertiliser. The limit of large  $q$  corresponds to the 1D BER recommendation. When organic matter is cheap, increase in profit will be limited by practical limitations of applying large amounts of OM.

#### 4. Discussion

Our methodology describes a means to put the multi-year response of crops to more than one input on a sound rational basis. The extension of the well-known break-even ratio to the economic response of crops to applications of organic matter during several years as well as to applications of  $N$  is a valuable addition to the farmer's and agronomist's recipe book. A second input such as organic matter as well as an extended time-frame bring still more factors into play such as the year-to-year change in the price of the OM. For these reasons it is difficult to present a simple table of BER values that suggest how more or less  $N$  a farmer should apply in relation to the price of wheat or fertiliser as it is done in fertiliser guidance such as the AHDB guide. The cost of OM and the time-frame also need to be taken into account.

In practice, progress may be made if we assume that there exists a kind of equilibrium that can be achieved dynamically by adding OM to soils leading to a soil carbon build-up. In the framework developed here, this equilibrium of yield-enhancing carbon is determined by Eqs. (25)–(26). To reach this equilibrium state, our analysis suggests applying the equilibrium amounts ( $U^*$ ,  $V^*$ ) of fertiliser and OM amendments. As shown in A where we study the consequences of bounded input rates (Figs. A.1, A.2, A.4), the profit maximising optimum trajectory (Sec. 3.2.2, Fig. 4) can be approximated by applying the amount  $U^*$  of fertiliser every year for the whole cultivation period  $T$ , whilst applying amendments at the  $V^*$  level for  $t^*$  years. This is the rule-of-thumb strategy that we propose (Fig. A.4). Disregarding year to year variation in weather, the 'exact' amounts ( $U^*$ ,  $V^*$ ) and timetable of application of amendment depend on the decay constants ( $k$ ,  $\kappa$ ), which are soil (and crop) properties but can be determined in principle using the methodology described in Sec. 2.3. It may be possible that such a steady-state is related to the equilibrium level of the amount of organic matter that can be built up in soil. But this requires further research.

The analysis and procedure presented in this article is intended to build on the existing guidance that is based on economic optima. However, at the time of writing the economics of organic amendment in terms of consistent pricing is unclear. Prices can vary from zero to considerably more than we suggest. Our prices factor in transport and spreading costs which are considerable because most amendments contain substantial amounts of water that bulks up the product and which also costs money to transport. Acquisition prices and spreading costs are not normally included in the nitrogen costs. Fertiliser is a dry product so that delivery can be factored into a price uniformly around the country. In general application costs are not included in current fertilizer guidance.

There can be little doubt that measuring the increase in yield that comes about as a result of amending soil with organic matter is difficult. Hijbeek et al. (2017) went as far as to conclude that there was no or little increase in yield on amending soil over and above what could be accounted for by the extra minerals the amendments contained. That is not the case in the WOM experiment. Here, nutrients including  $N$  were carefully accounted for and in earlier work (Mattingly, 1974) used explicitly to adjust the response curve  $N$  axis and so eliminate any effect of added mineral  $N$  from the amendment on yield response. There is little doubt that the yields are variable, however, and even under the carefully controlled conditions in the WOM experiment this variability makes it difficult to fit models and so extract important parameters of interest such as the rate of build-up and decline of the yield-enhancing effect of added OM. The data from the second phase of the WOM experiment (Fig. 2(b)) have been useful in this respect. As more data is

collected this should become possible to refine the methodology proposed here. We do not know why Hijbeek et al. (2017) found little response of crops to OM. It may be that their otherwise extensive survey of crops did not include crops from the UK. The UK's maritime position and growing season that continues through the winter or that starts early in spring may in some ways account for the different observations.

The methodology developed here allows a rationale for pricing field fertility from the concept of the Lagrange multipliers interpreted as the shadow prices of nitrogen and carbon, namely  $\lambda_t$  and  $\mu_t$ . In statics, as hinted in Sec. 2.4, the Lagrange multipliers represent the price of a unit increment in fertility, quantified in terms of yield-enhancing power of soil nitrogen and carbon, that corresponds to an increment in profit. At the BER, the cost of a unit increase in fertility just balances the marginal (revenue) product from the resulting increase in yield as is well-known. In dynamics (Sec. 2.5), we found that optimal trajectories are governed by a dynamical equilibrium resulting from the balance between inputs and annual losses assumed from the recurrence equations (16). The system adapts itself automatically to the internal dynamics of fertility such that the shadow prices marginal products of nitrogen and carbon, namely  $\lambda_t$  and  $\mu_t$ , are equal to their respective marginal costs ( $c$ ,  $q$ ) as long as fertiliser inputs and organic amendments are supplemented at the rates ( $U^*$ ,  $V^*$ ). However, amendments must be stopped towards the end of the cultivation horizon so that the OM shadow price of carbon  $\mu_T$  is equal to the marginal product for carbon allowed by the state of fertility in the final year  $T$  (i.e. the boundary conditions in Eq. (21)). We propose to define the value of the residual of field fertility from the terminal shadow price of carbon  $\mu_T$ , which our methodology computes. Alternatively, the cost of fertility could be evaluated from  $\xi_T = q - \mu_T$  (Sec. 3.2.2, (30)). All in all, along an optimal trajectory, the shadow prices of fertility ( $N$  or  $C$ ) never exceed the marginal costs of fertiliser and organic amendments, the schedule and level of amendments being optimised so that fertility remains at its optimum value to maximise the overall profit. This contrasts with the constrained case where fertiliser and organic amendment applications are limited as explained in A.

#### 5. Conclusion

Using the idea of a nutrient response curve seen as a production function, we have demonstrated how to compute time-dependent optimal strategies for organic matter applications that take account of how yields depend on the evolution of organic amendments and how long the associated benefits persist. It seems clear that, apart from the first and final six years (for Woburn) of a cultivation period, it makes sense to apply a constant rate of organic amendment to soil determined by the dynamic equilibrium of the yield-enhancing carbon provided by the amended soil organic matter. This rate will depend on the nature of the material, its longevity in soil and the economics of its acquisition and spreading.

We have showed that the fertility levels and inputs scheduled along such optimal trajectories are strongly governed by the rate of loss,  $1 - \kappa$ , of the yield-enhancing carbon (Figs. 2, 4). This is no surprise, since this is a key assumption underlying our approach. However, despite the simplicity of our 'soil fertility dynamical model' (uncoupled linear recurrence Eq. (16)), our approach captures the essence and reveals the complexity of the dynamics of fertility. It clearly demonstrates that the change in time of fertility cannot be overlooked in developing optimal guidance in the application of fertilisers that persist in soil and organic amendments to crops.

Key to our analysis is the assumption that there exists an equilibrium that is dynamically achieved by adding organic matter to soils leading to a soil yield-enhancing carbon build-up. The optimal control methodology takes advantage of this accumulation of fertility and its relatively slow decay, compared to the dynamics of applied nitrogen. Combined with our extension of the concept of nutrient response curve to organic matter, we can describe organic amendments as a long-term investment in soil fertility whose associated shadow price allows a rationale for its



economic valuation. With this respect, the method also lends itself to the valuation of land in relation to any residual fertility remaining should a farmer needs to sell land or give up a tenancy part way through a trajectory such as illustrated in Figs. 4 and 5. Calls have been made for land — especially rental land — to carry a kind of passport. Our optimal control methodology suggests a way of quantifying any residual value in land that result from management practices such as the application of FYM during tenancy.

**Declaration of Competing Interest**

The authors declare that they have no known competing financial interests or personal relationships that could have appeared to influence the work reported in this paper.

**Data availability**

Data will be made available on request.

**Appendix A. Effect of bounded input rates**

*Formulation*

The optimal trajectory that we described in the main body of the article (Fig. 4) is specific to the case where there is no additional constraint on the control variables  $U_b, V_b$ , apart from being non-negative. By contrast, interesting cases of practical importance arise when fertiliser and organic amendments applications are limited, for instance because of environmental regulations (NVZ rules) or practical reasons. Mathematically, this means that the domain of admissible controls is bounded. A simple example of such domains is the rectangular domain

$$\Omega(U, V) = \{(U_t, V_t) \in \mathbb{R}_+^2 \mid U_t \leq U, V_t \leq V\}, \tag{A.1}$$

where  $U$  and  $V$  represent the maximum input rates of nitrogen and carbon which are permitted to be applied each season. (Note that these maximum rates could be made time-dependent for more generality if necessary.) The domain  $\Omega$  is often referred to as the control set and the conditions  $0 \leq U_t \leq U$  and  $0 \leq V_t \leq V$  as *inequality constraints*. A boundary of the control set is said to be active whenever a control variable is equal to one of the endpoints of the intervals defining  $\Omega$ . Typical problems to solve are to find critical times at which an optimal trajectory hits or leaves the boundaries of the control

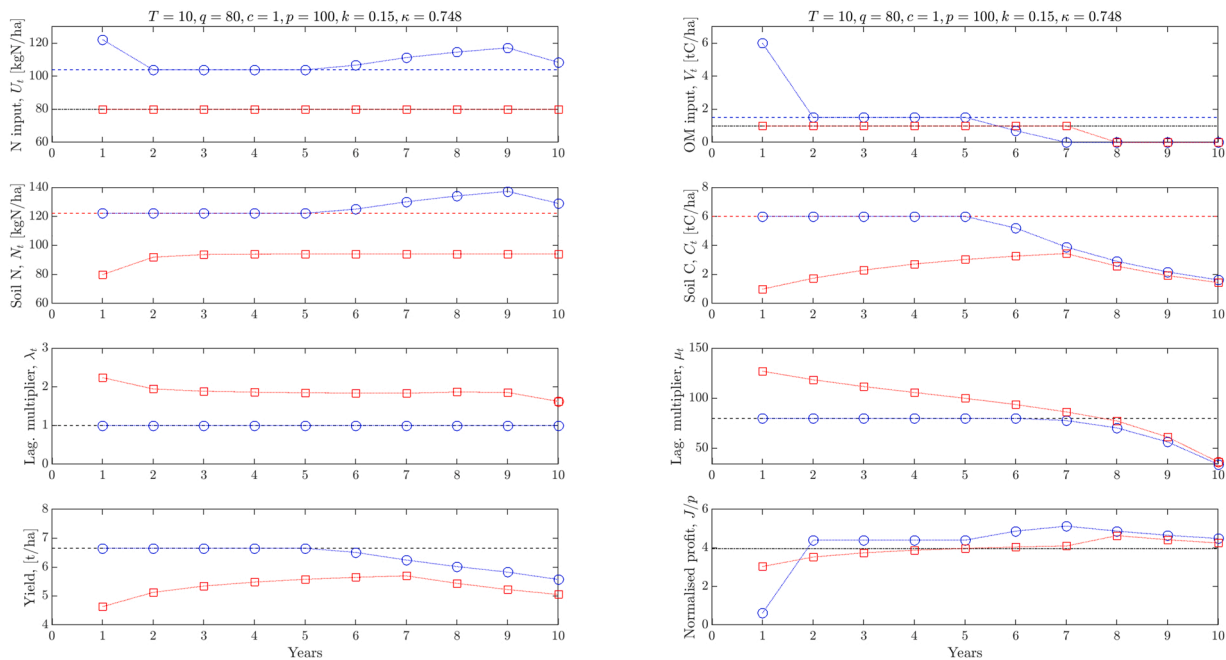


**Fig. A.1.** Low carbon input: comparison of an input-limited optimal trajectory (red,  $\square$ ) with the unconstrained optimal trajectory (blue,  $\circ$ ) (as in Fig. 4) for inputs limited to  $U = 80$  kg N/ha,  $V = 1.0$  t C/ha. Note that the input-limited trajectory has inputs locked on the limits of the control set  $\Omega = [0,80] \times [0,1]$ . Parameter values:  $T = 10$  yr,  $q = 80$  £ /t C,  $c = 1$  £ /kg N,  $p = 100$  £ /t,  $k = 0.15$ ,  $\kappa = 0.748$ ,  $N_0 = C_0 = 0$ .

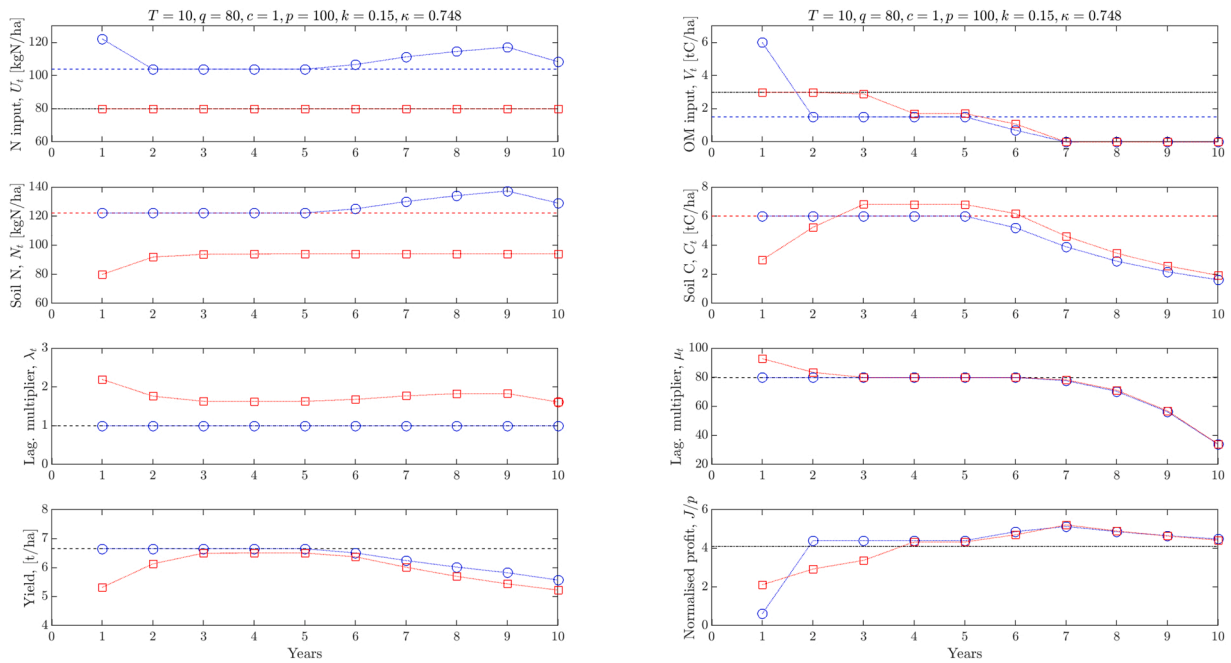


**Fig. A.2.** Moderate carbon input: comparison of an input-limited optimal trajectory (red,  $\square$ ) with the unconstrained optimal trajectory (blue,  $\circ$ ) (as in Fig. 4) for inputs limited to  $U = 80$  kg N/ha,  $V = 3$  t C/ha. Note that the input-limited trajectory has inputs not locked on the limits of the control set  $\Omega = [0,80] \times [0,3]$ . The level of amendments allows for reaching the equilibrium. The input-limited trajectory tends to the unconstrained dynamics. Parameter values:  $T = 10$  yr,  $q = 80$  £ /t C,  $c = 1$  £ /kg N,  $p = 100$  £ /t,  $k = 0.15$ ,  $\kappa = 0.748$ ,  $N_0 = C_0 = 0$ .

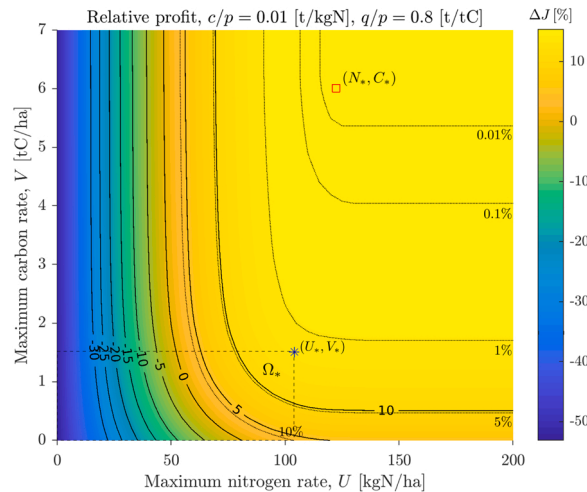


**Fig. A.3.** Normalised (relative) profit ( $\Delta J$ ) iso-contours for input-limited optimal trajectories. The x and y axes express the maximum (constrained) inputs for N and C respectively. The iso-lines with percentages highlight the distance to achieving maximum profit, which is given by the unconstrained optimal trajectory. The blue symbol \* highlights the location of the equilibrium input rates  $(U^*, V^*)$ . The red symbol  $\square$  corresponds to the location of the first year input rates in the unconstrained optimal trajectory. If the point  $(N^*, C^*)$  belongs to the control set  $\Omega$  defined in (A.1), the input-limited trajectory corresponds to the unconstrained optimal trajectory discussed in Sec. 3.2.2. The dashed line rectangular domain  $\Omega^*$  represents the control set of the input-limited ‘rule-of-thumb’ optimal trajectory. Parameter values:  $T = 10$  yr,  $q = 80$  £ /t C,  $c = 1$  £ /kg N,  $p = 100$  £ /t,  $k = 0.15$ ,  $\kappa = 0.748$ ,  $N_0 = C_0 = 0$ .

set. In our case, such times correspond to switches between applying or withholding OM.

Mathematically, the two inequality constraints must be associated with two Lagrange multipliers and must be included into the Lagrangian function (19) defined in Sec. 2.5.2 by adding the term  $\sum_{t=1}^T [\gamma_t(U - U_t) + \eta_t(V - V_t)]$ . In turn, this modification of the Lagrangian function implies that expressions in (23) become

$$\gamma_t = \lambda_t - c + \zeta_t, \quad \eta_t = \mu_t - q + \xi_t, \tag{A.2}$$

while the slackness conditions

$$\gamma_t \geq 0, \quad \gamma_t(U - U_t) = 0, \quad \eta_t \geq 0, \quad \eta_t(V - V_t) = 0, \tag{A.3}$$

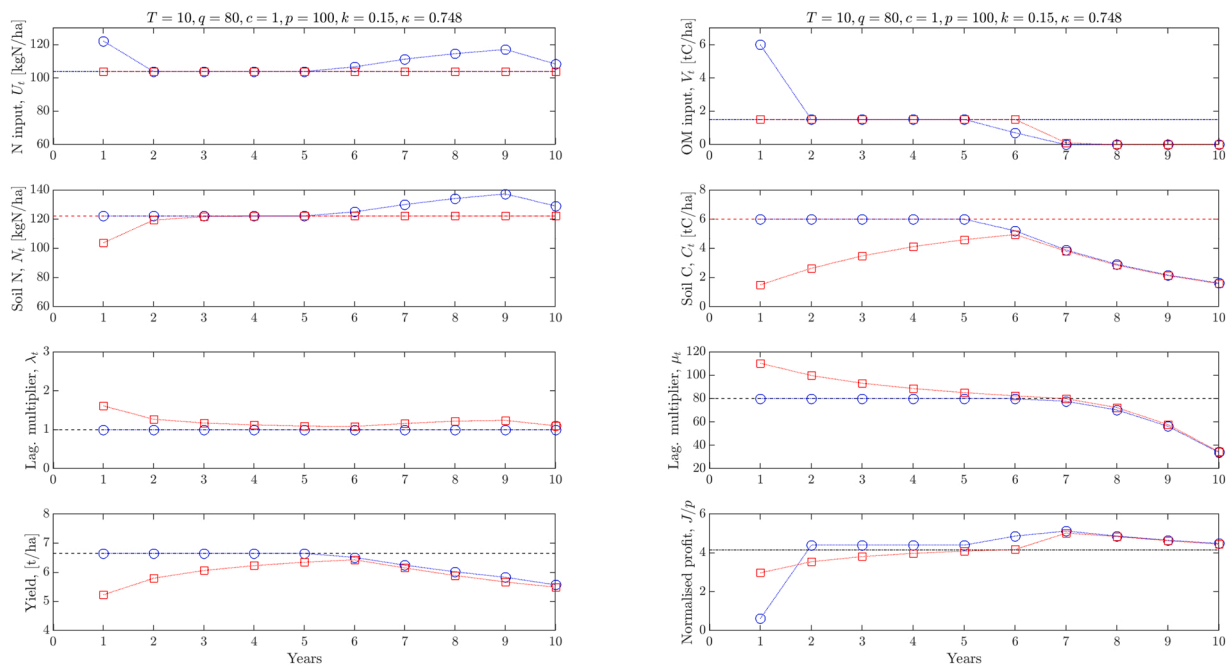


**Fig. A.4.** Rule of thumb strategy: comparison of an input-limited optimal trajectory (red,  $\square$ ) with the unconstrained optimal trajectory (blue,  $\circ$ ) (as in Fig. 4) for inputs limited to  $U = U^*$  kg N/ha,  $V = V^*$  t C/ha. The equilibrium input values ( $U^*$ ,  $V^*$ ) are defined in Sec. 2.6, Eqs. (25)–(26). Parameter values:  $T = 10$  yr,  $q = 80$  £ /t C,  $c = 1$  £ /kg N,  $p = 100$  £ /t,  $k = 0.15$ ,  $\kappa = 0.748$ ,  $N_0 = C_0 = 0$ .

must be added to the complementary slackness conditions (24). From (24), we recall that the multipliers  $\zeta_t$ ,  $\xi_t$  are zero if the fertiliser and amendments are applied ( $U_t \neq 0$ ,  $V_t \neq 0$ ).

*Conditions for application*

It follows from (A.3) that expressions (A.2) reduce to

$$\gamma_t = \lambda_t - c > 0, \quad \eta_t = \mu_t - q > 0, \tag{A.4}$$

whenever the boundaries of the control set are active with  $U_t = U$ ,  $V_t = V$ . That is fertiliser and organic amendments are applied at their maximum permitted rates. Inequalities (A.4) imply that the nitrogen and carbon shadow prices  $\lambda_t$  and  $\mu_t$  become larger than the nitrogen and carbon prices  $c$  and  $q$ . This contrasts strongly with the unbounded optimal trajectory shown in Figs. 4 and 6 for which the shadow prices are at their dynamic BER values  $\lambda_t \equiv c$ ,  $\mu_t \equiv q$  for seasons  $t \leq t^*$ . The constrained case (A.4) is reminiscent of the two-dimensional static case (15) where inputs belong to the profitability domain  $\bar{\Omega}$  and  $\gamma, \eta > 0$  (Fig. 3(b)). In this case, the profit could be increased further if one were to increase the rates of inputs (Secs. 2.4.2, 3.2.1). In the input-limited dynamic case, we expect that a constrained optimal trajectory (while still maximising profit under the constraint of limited inputs) will not lead to the absolute maximum of profit pertaining to the system, which would be the profit associated with the unconstrained optimal trajectory described in Sec. 3.2.2. The Lagrange multipliers  $\gamma_t$ ,  $\eta_t$  quantify dynamically how far an input-limited optimal trajectory is from the unconstrained optimal trajectory we described at length in this article. The multipliers  $\gamma, \eta$  play the same role in statics, once inputs are limited. The same reasoning applies for nitrogen (see below).

*Discontinuation of amendments*

When organic amendments are stopped  $V_t = 0$ , we have  $\xi_t > 0$  and  $\eta_t = 0$  necessarily from (24) and (A.3). In turn the carbon shadow price is  $\mu_t = q - \xi_t < q$ , as for the unconstrained dynamics (23). As  $\mu_t$  is below its dynamic BER value, there is no margin left to organic matter applications, which have become too expensive. This shows as a decreasing profit for the subsequent seasons (Figs. A.1, Figs. A.2).

*Examples*

Figs. A.1 and A.2 show input-limited optimal trajectories both with  $U = 80$  kg N/ha but with different maximum organic matter input rates  $V = 1$  and  $V = 3$  t C/ha ( $\square$  lines). The unconstrained optimal trajectory ( $\circ$  lines) is shown for comparison. Here nitrogen must still be applied for the whole period of ten years, but its input rate is locked at its maximum allowed value  $U$ . When  $V \leq V^*$  (Fig. A.1), organic matter is also applied at its constant maximum rate  $V$  until the amendments discontinuation-time is reached. Note that, in this instance, it is two more years than for the unconstrained case (i.e.  $t^* = 7$  years instead of 5). By contrast, because amendments are bounded to a value less than the dynamic equilibrium  $V^*$ , the soil carbon cannot be topped-up to its dynamic equilibrium value from year one with a large initial amendment. Instead, the yield enhancing soil carbon increases gradually towards a new dynamic equilibrium  $C_+ = V/(1 - \kappa) < C^*$ . As the soil carbon rises, yield increases and the organic matter shadow price  $\mu_t$  decreases as a result. The discontinuation of organic matter amendments is then associated with its shadow price  $\mu_t$  crossing the dynamic BER value  $q$ . It has become too expensive to add carbon compared to the revenue generated from the extra yield, as would be the case for the unconstrained trajectory. The OM boundary of the control set becomes inactive, and amendments are discontinued. When  $V \geq V^*$  (Fig. A.2), similar dynamical effects are observed.

However, the increase of the soil carbon towards its equilibrium is faster because more carbon is available to be put into the system. In Fig. A.2, the OM boundary is active for two years, then amendments are slightly reduced to reach  $V^*$  until the discontinuation time  $t^*$ . Interestingly, we see that  $\mu_t$  decays towards its dynamic BER value  $q$  after this initial phase of two years. The rest of this input-limited trajectory is very close to the unconstrained optimal trajectory and behaves in a similar fashion. Note that in this situation, the soil carbon can overshoot the unlimited-input equilibrium  $C^*$ . The soil carbon equilibrium is different because the nitrogen  $U < U^*$  does permit the soil nitrogen to reach its unlimited equilibrium  $N^*$ . Regarding nitrogen, for all seasons,  $\lambda_t > c$  and nitrogen is applied at the maximum permitted rate  $U_t \equiv U$ . Because the dynamics of nitrogen are fast ( $k \ll 1$ ), the soil nitrogen quickly reaches the dynamic equilibrium  $N_+ = U/(1 - k) < N^*$ . The unlimited-input dynamic equilibrium  $N^*$  cannot be attained as  $U < U^*$ . Note however that the scheduling of nitrogen inputs is much simpler in the input-limited case: a constant rate should be applied each year, compared to the unconstrained case in which rates increase towards the end of the cultivation horizon.

*Profit iso-contour map*

With the two examples described previously, we saw that input-limited optimal trajectories strongly depend on the boundaries of the control set. In our case, these boundaries are simple and determined by the bounds  $U, V$  of the control set  $\Omega(U, V)$ . Looking at any such optimal input-limited trajectories as parameterised by these bounds, we computed the total profit for a total period of  $T = 10$  years while varying these bounds. Fig. A.3 shows in the  $(U, V)$ -plane the relative profit ( $\Delta J = 100(\bar{J}/J_+ - 1)$ ) iso-contour map synthesising the 10-year profit that is achievable for a given set of the economic parameters  $p, c, q$  relatively to the 1D BER profit with no OM input. Compared to the iso-contour map for the static profit optimisation problem (Fig. 3), the profit iso-lines have an elbow shape and do not close up to form a well identified apex of profit. Instead, the profit saturates towards the top-right corner of the diagram in Fig. A.3 and the topography of the profit landscape flattens when the control set limits  $U, V$  are large enough. This is because, as we saw in the simulation presented in Fig. A.2, the input-limited optimal trajectories converge towards the unconstrained optimal trajectory as the bounds  $U, V$  become larger and larger. In turn, the profit generated converges to the absolute maximum given by the unconstrained optimal trajectory. We recall that the unconstrained trajectory is characterised by input rates in the first year equal to the dynamic equilibrium values of nitrogen and carbon, i.e.  $(U_1, V_1) = (N^*, C^*)$ . When the limits of the control set  $\Omega$  exceed this level, input-limited trajectories have fully converged to the unconstrained optimal trajectory. In this situation, the control set can be seen to be unbounded. This behaviour also explains the right-angle elbow shape of the profit iso-contours. In the situation where  $U \gg N^*$  (resp.  $V \gg C^*$ ), the iso-contours are horizontal (resp. vertical) because the nitrogen inputs (resp. organic amendments) tend to the corresponding unconstrained optimal trajectory. From this, we can conclude that stringent limitations imposed on nitrogen applications can be compensated by organic matter amendments, still allowing similar orders of magnitude in profit. Conversely, at high nitrogen inputs that approximate the guidance (AHDB) BER rate, significant gains in profit ( $> 10\%$ ) could be achieved from moderate applications of organic matter ( $< 2$  t C/ha). In Fig. A.3, we highlight five iso-lines (dotted black lines) representing a profit reduction of 0.01%, 0.1%, 1%, 5% and 10% from the absolute maximum profit in unconstrained dynamics. This shows that a large corner of the  $(U, V)$ -plane, is delimited by the 1% iso-line. In this region, input-limited trajectories are all equivalent in terms of profit; only marginal gains of less than 1%, can be generated. Interestingly, numerical calculation shows that the input-limited optimal trajectory corresponding to the control set  $\Omega^* = \Omega(U^*, V^*)$  defined by the dynamical BER rates (o-blue line in Fig. A.4) reaches a profit that is only about 2% less than the absolute maximum. For practical reasons, it seems to us that this optimal trajectory is the simplest and the best to follow because the fertiliser application rate is constant and fixed to  $U^*$  every year, while the amendments rate is fixed to  $V^*$  until the discontinuation time is reached (Fig. A.2). This strategy would generate an increase in profit about 14% more than a BER recommendation with no OM inputs.

**B. Linear-plus-exponential response curve and model selection**

The idea of modifying the maximum crop response rate  $B$  to  $B(1 + y)$  to include the yield-enhancing power of farmyard manure into a nitrogen response curve (Sec. 2.3) can be done for a 'lexp' response curve in a very similar fashion, assuming for simplicity

$$Y(N, y) = a[1 - e^{-b(1+y)(N_s+N)}] - c_1 N. \tag{B.1}$$

As for the reciprocal model (3), the slope of the response for low N rates changes because of the level organic amendments via the proxy variable  $y$ . The

**Table B.1**  
Parameter values for the linear-plus-exponential model (B.1) (FYM).

Parameters	$a$	$b$	$N_s$	$c_1$	$\kappa$	$y_{86}$	$v$	$C_s$	$C_{86}$
Units	t/ha	t/kgN	kgN/ha	t/kgN	—	—	—	tC/ha	tC/ha
Values	10.8	0.00599	30.8	0.0131	0.755	1.29	0.387	10.0	12.9

**Table B.2**  
Reciprocal model (3) with downturn.

Parameters	Estimate	Std. Error	t value	Pr ( $>  t $ )
$A$	1.219E+ 01	3.024E+ 00	4.033	6.35E-05 * **
$B$	7.045E-02	1.076E-02	6.546	1.43E-10 * **
$N_s$	2.926E+ 01	7.341E+ 00	3.985	7.71E-05 * **
$\alpha$	1.050E+ 03	4.197E+ 02	2.501	0.0127 *
$\kappa$	7.484E-01	4.303E-02	17.391	< 2E-16 * **
$y_0$	2.142E+ 00	8.573E-01	2.498	0.0128 *
df	516			
RSE	1.511			
AIC	1920.528			



**Table B.3**  
Reciprocal model (3) without downturn.

Parameters	Estimate	Std. Error	t value	Pr ( >  t )
A	7.945E+ 00	5.562E-01	14.284	< 2E-16 ***
B	7.671E-02	1.261E-02	6.083	2.3E-09 ***
$N_s$	2.867E+ 01	7.702E+ 00	3.723	2.18E-04 ***
$\kappa$	7.2012E-01	4.827E-02	14.919	< 2E-16 ***
$y_0$	4.030E+ 00	1.559E+ 00	2.584	0.010031 *
df	517			
RSE	1.516			
AIC	1922.633			

**Table B.4**  
Linear-plus-exponential model (B.1) with downturn.

Parameters	Estimate	Std. Error	t value	Pr ( >  t )
a	1.077E+ 01	1.465E+ 00	7.349	7.85E-13 ***
b	5.994E-03	7.795E-04	7.690	7.51E-14 ***
$N_s$	3.079E+ 01	6.875E+ 00	4.479	9.25E-06 ***
$c_1$	1.306E-02	4.305E-03	3.033	0.00254 **
$\kappa$	7.553E-01	4.010E-02	18.835	< 2E-16 ***
$y_0$	1.289E+ 00	3.892E-01	3.312	0.00099 ***
df	516			
RSE	1.519			
AIC	1925.531			

**Table B.5**  
Linear-plus-exponential model (B.1) without downturn.

Parameters	Estimate	Std. Error	t value	Pr ( >  t )
a	7.365E+ 00	4.520E-01	16.295	< 2E-16 ***
b	5.290E-03	8.261E-04	6.403	3.42E-10 ***
$N_s$	6.033E+ 01	1.182E+ 01	5.104	4.68E-07 ***
$\kappa$	7.463E-01	4.436E-02	16.822	< 2E-16 ***
$y_0$	2.137E+ 00	6.470E-01	3.303	0.00102 **
df	517			
RSE	1.532			
AIC	1933.562			

**Table B.6**  
Akaike's model performance estimates (Burnham and Anderson, 2002).

Model	AIC difference $\delta_i$	Likelihood $\mathcal{L}_i$	Akaike weight $w_i$	Evidence ratio $w_1/w_i$
1. Reciprocal model (3) with downturn	0	1	0.698	—
2. Reciprocal model (3) without downturn	2.105	0.3491	0.244	2.9
3. <i>lexp</i> model (B.1) with downturn	5.003	0.0820	0.057	12.3
4. <i>lexp</i> model (B.1) without downturn	13.034	0.0015	0.001	698

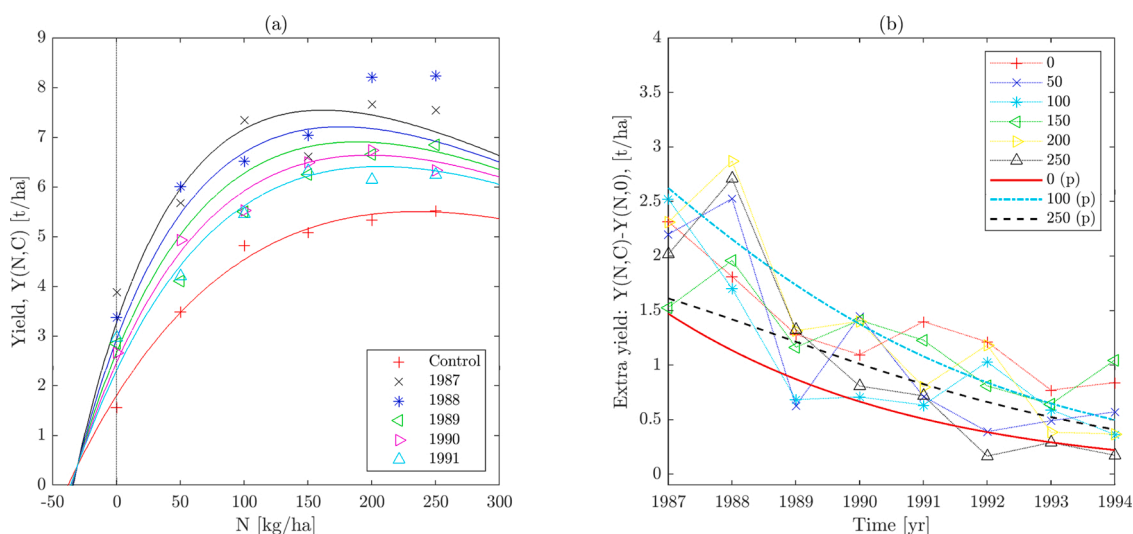


**Fig. B.1.** Response curve and extra yield for the linear-plus-exponential model (B.1).

fitted parameter values are given in Table B.1.

The full results of the nonlinear least-squares analysis with the R routine NLS of the reciprocal (3) and 'lexp' (B.1) models, with or without downturn, are summarised in Tables B.2, B.3, B.4, B.5. All candidate models performed well for the Woburn dataset. Model selection based the Akaike information criterion (AIC) (Burnham and Anderson, 2002) is however in favour of the reciprocal response curve (3) with a downturn (Table B.2) because its AIC is the smallest.

When comparing the performance of models with this criterion, it is the relative values of AICs quantified by the differences  $\delta_i = AIC_i - AIC_{\min}$  that matter. Given the data and a set of models, the plausibility of each model of being the (Kullback-Leibler) best model follows from the relative strength of evidence for each model  $i$ , which is estimated by the likelihood  $\mathcal{L}_i \propto \exp(-\delta_i/2)$ . The model probabilities are then given by the Akaike weights  $w_i = \mathcal{L}_i / \sum_j \mathcal{L}_j$ . From these estimates (Table B.6), we can conclude that the 'lexp' models lose some amount of information, and hence, fail to capture some explainable variation in the Woburn data. By contrast, from its Akaike weight (Table B.6), we find that there is about 70% chance that the reciprocal response curve (3) with a downturn is the best model of the four, given the data that we use here.

Fig. B.1

## C. Definition of the key variables and parameters

See Table C.1.

Table C.1

List of key variables and parameters used in the text. (Note that  $\lambda_t$  and  $\mu_t$  can exceed their upper bounds  $c$  and  $q$  when the input rates are bounded, see A.).

Variable, parameter	Definition	Units	Values
$T$	Cultivation horizon, total number of seasons	yr	10
$t \in [1, T]$	Season index	yr	—
$t_s$	Organic amendment discontinuation time	yr	5
$Y$	Crop yield (assumed function of $(N_t, C_t)$ )	t/ha	[0,9]
$Y_N := \partial Y / \partial N$	Partial derivative of $Y$ with respect to $N$	t/kg N	—
$Y_C := \partial Y / \partial C$	Partial derivative of $Y$ with respect to $C$	t/t C	—
$A$	Theoretical maximum yield	t/ha	12.2
$B$	Maximum crop response rate	t/kg N	0.0705
$\alpha$	Growth inhibitor coefficient	kg N/ha	1050
$N_s$	Soil indigenous (native) nitrogen	kg N/ha	29.3
$C_s$	Yield-enhancing carbon of reference	t C/ha	5.95
$N_t$	Soil available nitrogen content, state variable	kg N/ha	[100,140]
$C_t$	Soil yield-enhancing carbon content, state variable	t C/ha	[0,6]
$y_t \equiv C_t / C_s$	Organic matter yield-enhancing proxy, state variable	—	[0,1]
$U_t$	Nitrogen application rate, control variable	kg N/ha	[100,130]
$V_t$	Carbon application rate, control variable	t C/ha	[0,6]
$v_t \equiv V_t / C_s$	Dimensionless organic matter application rate, control variable	—	[0,1]
$k$	N decay (carry-over) constant	—	0.15
$\kappa$	C,y decay (carry-over) constant	—	0.748
$N_e$	Equilibrium soil nitrogen content	kg N/ha	122
$C_e$	Equilibrium soil carbon content	t C/ha	6.01
$U_e$	Dynamic BER nitrogen application rate	kg N/ha	104
$V_e$	Dynamic BER farmyard manure application rate	t C/ha	1.52
$p$	Crop price	£ /t	100
$c$	Nitrogen fertiliser price	£ /kg N	1
$q$	Farmyard manure (FYM) price	£ /t C	{37, 80}
$J$	Total profit over $T$ seasons	£ /ha	—
$L$	Lagrangian function	£ /ha	—
$\lambda_t$	Nitrogen shadow price, nitrogen dynamics Lagrange multiplier	£ /kg N	[0, c]
$\mu_t$	Carbon shadow price, carbon dynamics Lagrange multiplier	£ /t C	[0, q]
$\nu_t$	Lagrange multiplier to ensure $N_t \geq 0$	£ /kg N	$\geq 0$
$\nu_t$	Lagrange multiplier to ensure $C_t \geq 0$	£ /t C	$\geq 0$
$\zeta_t$	Lagrange multiplier to ensure $U_t \geq 0$	£ /kg N	[0, c]
$\xi_t$	Lagrange multiplier to ensure $V_t \geq 0$	£ /t C	[0, q]

## References

- Addiscott, T.M., Whitmore, A.P., 1987. Computer simulation of changes in soil mineral nitrogen and crop nitrogen during autumn, winter and spring. *J. Agric. Sci.* 109, 141–157. <https://doi.org/10.1017/S0021859600081089>.
- Addy, J., Ellis, R., Macdonald, A., Semenov, M., Mead, A., 2020. Investigating the effects of inter-annual weather variation (1968–2016) on the functional response of cereal grain yield to applied nitrogen, using data from the rothamsted long-term experiments. *Agric. For. Meteorol.* 284, 107898 <https://doi.org/10.1016/j.agrformet.2019.107898>.
- Addy, J., Ellis, R., Macdonald, A., Semenov, M., Mead, A., 2021. Changes in agricultural climate in south-eastern england from 1892 to 2016 and differences in cereal and permanent grassland yield. *Agric. For. Meteorol.* 308–309, 108560 <https://doi.org/10.1016/j.agrformet.2021.108560>.
- Albano, X., Whitmore, A., Sakrabani, R., Thomas, C., Sizmur, T., Ritz, K., Harris, J., Pawlett, M., Watts, C., Haeefe, S., 2022. Effect of organic amendments on yields, yield potential and nitrogen use efficiency in a cereal-based cropping system. *Sub-judice*.
- Balmukand, B., 1928. Studies in crop variation: V. The relation between yield and soil nutrients. *J. Agric. Sci.* 18, 602–627. <https://doi.org/10.1017/S0021859600009199>.
- Barnes, A., Greenwood, D.J., Cleaver, T.J., 1976. A dynamic model for the effects of potassium and nitrogen fertilizers on the growth and nutrient uptake of crops. *J. Agric. Sci.* 86, 225–244. <https://doi.org/10.1017/S002185960005468X>.
- Beattie, A., 2020. *The Farm Management Handbook 2020/21*. SAC Consulting.
- Bellman, R., 2013. *Dynamic Programming*. Dover.
- Bradbury, N.J., Whitmore, A.P., Hart, P.B.S., Jenkinson, D.S., 1993. Modelling the fate of nitrogen in crop and soil in the years following application of  $^{15}\text{N}$ -labelled fertilizer to winter wheat. *J. Agric. Sci.* 121, 363–379. <https://doi.org/10.1017/S0021859600085567>.
- Burnham, K., Anderson, D., 2002. *Model Selection and Multimodel Inference: A Practical Information-Theoretic Approach*. Springer, <https://doi.org/10.1007/b97636>.

- Chiang, A., 1984. *Fundamental Methods of Mathematical Economics*. Economics Series, 3rd ed., McGraw-Hill International Editions.
- Clark, C., 1976. *Mathematical Bioeconomics: The Optimal Management of Renewable Resources*. Wiley-Interscience.
- Dewar, A., 2017. The adverse impact of the neonicotinoid seed treatment ban on crop protection in oilseed rape in the united kingdom. *Pest Manag. Sci.* 73, 1305–1309. <https://doi.org/10.1002/ps.4511>.
- Eklind, Y., Kirchmann, H., 2000. Composting and storage of organic household waste with different litter amendments. i: carbon turnover. *Bioresour. Technol.* 74, 115–124. [https://doi.org/10.1016/S0960-8524\(00\)00004-3](https://doi.org/10.1016/S0960-8524(00)00004-3).
- George, B., 1984. Design and interpretation of nitrogen response experiments, in: Nitrogen requirement of cereals, Agricultural Development and Advisory Service.133–148. ADAS Conference September 1982. London: HMSO.
- Greenwood, D., Wood, J., Cleaver, T., Hunt, J., 1971. A theory for fertilizer response. *J. Agric. Sci.* 77, 511–523. <https://doi.org/10.1017/S0021859600064595>.
- Hijbeek, R., van Ittersum, M., tenBerge, H., Gort, G., Spiegel, H., Whitmore, A., 2017. Do organic inputs matter—a meta-analysis of additional yield effects for arable crops in europe. *Plant Soil.* <https://doi.org/10.1007/s11104-016-3031-x>.
- Intriligator, M., 1971. *Mathematical Optimization and Economic Theory*. Prentice-Hall.
- Johnston, A., Poulton, P., Coleman, K., 2009. Soil organic matter: Its importance in sustainable agriculture and carbon dioxide fluxes. *Adv. Agron.* 101, 1–57. [https://doi.org/10.1016/S0065-2113\(08\)00801-8](https://doi.org/10.1016/S0065-2113(08)00801-8).
- Macdonald, A., Poulton, P., Clark, I., Scott, T., Glendining, M., Perryman, S., Storkey, J., Bell, J., Shield, I., Mcmillan, V., Hawkins, J., 2019. Guide to the classical and other long-term experiments, datasets and sample archive.
- Mangasarian, 1969. *Nonlinear Programming*. McGraw-Hill.
- Mattingly, G., 1974. The Woburn Organic Manuring Experiment. I Design, Crop Yields and Nutrient Balance, 1964–72. Technical Report. Rothamsted Experimental Station Report for 1973.
- Mattingly, G., Johnston, A., Poulton, P., 1981–1994. Rothamsted Experimental Station - Yields of the Long-term Field Experiments. Technical Report. Rothamsted Research, UK. Section 86/W/RN/12 Organic Manuring. (<https://www.era.rothamsted.ac.uk/eradoc/books/2>).
- Neal, A., Bacq-Labreuil, A., Zhang, X., Clark, I., Coleman, K., Mooney, S.K.R., Crawford, J., 2020. Soil as an extended composite phenotype of the microbial metagenome. *Sci. Rep.* <https://doi.org/10.1038/s41598-020-67631-0>.
- Pontryagin, L., 1987. *Mathematical Theory of Optimal Processes*. Taylor & Francis.
- Powlson, D., Bhogal, A., Chambers, B., Coleman, K., Macdonald, A., Goulding, K., Whitmore, A., 2012. The potential to increase soil carbon stocks through reduced tillage or organic material additions in england and wales: A case study. *Agric., Ecosyst. Environ.* 146, 23–33. <https://doi.org/10.1016/j.agee.2011.10.004>.
- Putelat, T., Whitmore, A., Senapati, N., Semenov, M., 2021. Local impacts of climate change on winter wheat in great britain. *R. Soc. Open Sci.* 8, 201669 <https://doi.org/10.1098/rsos.201669>.
- RB209, 2022. Nutrient Management Guide (RB209). Agriculture and Horticulture Development Board. (<https://ahdb.org.uk/RB209>).
- Sage, A., White III, C., 1977. *Optimum Systems Control*. Prentice-Hall, Inc.
- Samuelson, P., 1980. *Economics*, 11th ed., McGraw-Hill.
- Sethi, S.P., 2019. *Optimal Control Theory: Applications to Management Science and Economics*. Springer. <https://doi.org/10.1007/978-3-319-98237-3>.
- Stewart, W., Roberts, T., 2012. Food security and the role of fertilizer in supporting it. *Procedia Eng.* 46, 76–82. <https://doi.org/10.1016/j.proeng.2012.09.448>. SYMPHOS 2011 – 1st International Symposium on Innovation and Technology in the Phosphate Industry.
- Stewart, W.M., Dibb, D.W., Johnston, A.E., Smyth, T.J., 2005. The contribution of commercial fertilizer nutrients to food production. *Agron. J.* 97, 1–6. <https://doi.org/10.2134/agronj2005.0001>.
- Thomas, C., Acquah, G., Whitmore, A., McGrath, S., Haeefe, S., 2019. The effect of different organic fertilizers on yield and soil and crop nutrient concentrations. *Agronomy* 9, 776. <https://doi.org/10.3390/agronomy9120776>.
- Thornley, J., 1976. *Mathematical Models in Plant Physiology: A Quantitative Approach to Problems in Plant and Crop Physiology*. Academic Press., London.
- Thornley, J., 1978. Crop response to fertilizers. *Ann. Bot.* 42, 817–826. <https://doi.org/10.1093/oxfordjournals.aob.a085521>.
- Thornley, J., Johnson, I., 1990. *Plant and Crop Modelling: A Mathematical Approach to Plant and Crop Physiology*. Oxford Science Publications, Clarendon Press.
- UNEP, 2022. Synthesis Report on the Environmental and Health Impacts of Pesticides and Fertilizers and Ways to Minimize Them. Technical Report. United Nations Environment Programme. (<https://wedocs.unep.org/xmlui/bitstream/handle/20.500.11822/38409/pesticides.pdf>).